Electronic Thesis and Dissertation Repository

8-13-2021 10:00 AM

Uncertainties in internal pressure of oil pipelines and implications for the reliability analysis

Yue Liu, *The University of Western Ontario*

Supervisor: Zhou, Wenxing, *The University of Western Ontario*
A thesis submitted in partial fulfillment of the requirements for the Master of Engineering
Science degree in Civil and Environmental Engineering
© Yue Liu 2021

Follow this and additional works at: https://ir.lib.uwo.ca/etd

Part of the Civil Engineering Commons, and the Risk Analysis Commons

Abstract

The internal pressure is the most important operational load for oil and gas pipelines. The maximum operating pressure (MOP) is the maximum pressure the pipeline is qualified to be operated according to a given standard. In deterministic fitness-for-service (FFS) assessment of in-service pipelines containing flaws such as corrosion defects and cracks, the remaining pressure containment capacity of the pipeline is evaluated and compared with MOP multiplied by a factor of safety to determine if immediate rehabilitation actions for the pipeline are necessary. However, the actual internal pressure of an in-service pipeline is however uncertain and fluctuates with time. Due to the significant difference in the compressibility of liquid and gas, the pressure fluctuation in liquid pipelines. This thesis characterizes the statistics for the internal pressure of oil pipeline and assesses the reliability performance based on the pressure variables.

In this study it is characterized the internal pressure (discharge and suction) probabilistic properties of a major crude oil transmission pipeline including its distribution of arbitrary-point-in-time and maxima pressure, auto-correlation, power spectral density and pressure range from rain flow counting. The conclusions provide information for reliability analysis considered the pressure to be a stationary stochastic process and it gives suggestions for fatigue analysis.

It is also investigated the reliability performance for corroding pipelines considering the pressure statistics obtained in the first study and compared with different pressure assumptions. This study provides a method to consider the internal pressure to be a stochastic process and gives evidence that a certain level of conservativeness is observed if the internal pressure is considered as a stochastic process instead of a random variable suggested in present literature.

Key word: Pipeline, internal pressure, statistics, reliability, simulation, stochastic process

Summary for Lay Audience

Pipeline system often faces with many kinds of threats. Therefore, a mitigate procedure to reduce the incident rate is the fitness-for-service assessment. Within this assessment, the internal pressure is a major aspect of the assessment. This assessment considers uncertainties of all the aspects that influence the failure of pipeline. Therefore, the uncertainty of the pressure is one of the key interests in this assessment. The statistical characterization of the internal pressure is often assumed to follow certain distribution in papers and code, however, the internal pressure for oil pipelines is much less sourced. The present study has collected internal pressure data from one pump station of an in-service oil pipeline and characterized basic features including not only the distribution, mean and standard deviation but also time-dependent features such as the correlation between pressures with different time lags. The statistics provide the researchers more options to incorporate internal pressure for oil pipeline specifically into future studies, for instance as time-independent or time-dependent in the reliability analyses, or fatigue crack failure assessment. The present study further investigates how different assumptions about the uncertainty in the internal affect the reliability analysis results for corroding pipelines.

Acknowledgement

First and foremost, I would like to express my sincere gratitude to my supervisor Professor Wenxing Zhou. Dr. Zhou's profound knowledge and great patience has opened the gate for me as a starter with no experience in research at all. His patience and kindness have never stopped for me the entire two years' study. It's been hard time unexpected to all of us when the pandemic hit London and the University had to shut down the campus. The research progress is seriously impacted as the working and social environment is locked at the same time. With limited help and much less opportunities of communication with friends and colleagues, Dr. Zhou's guidance becomes even invaluable. Our weekly online meeting keeps going all the way and this I believe is the main reason that my research process is carefully steered and guided in the right direction. I'm not sure if I could have opportunity to keep exploring the research path in the future, but I know in any ways, those skills and thinking will always accompany with me.

I would like to extend my appreciation to members of my thesis examination committee, Dr. Hong, Dr. Najafi and Dr. Mao for the time and efforts they put in reviewing my thesis, raising critical questions and assessments. I gratefully acknowledge the financial support provided by the Natural Sciences and Engineering Research Council of Canada (NSERC).

Special thanks to my colleagues in our research group, Dr. Ji Bao, Dr. Wei Xiang, Junxiong Lin, Ziming He, Haotian Sun, Haoyi Zhang and Yufei Shen, your encouragement and countless discussions gave me great support especially during this hard time.

My deepest gratitude to my parents and friends for their unconditional support, their encouragement has always inspired me when I need them. I hope one day I could repay their kindness.

Table of content

List of Figures

List of Tables

List of Abbreviations and Symbols

Abbreviations

CDF   cumulative distribution function

COV   coefficient of variation

CSA   Canadian Standards Association

FFS   fitness-for-service

FFT   fast Fourier transform

FORM   first ordered reliability method

FS   Design factor

IID   independent and identically distributed

ILI   inline inspections

ISCM   iterative spectral correction method

JSB   Johnson SB distribution

MCS   Monte Carlo simulation

MOP   maximum operating pressure

PDF   probability density function

PSD   power spectral density

PHMSA   Pipeline and Hazardous Material Safety Administration

SCC   stress corrosion cracking

SMYS   specified minimum yield strength

SMTS   specified minimum tensile strength

SORM   second ordered reliability method

Symbols

Chapter 2

p_{ae}	maximum internal pressure
t_n	nominal wall thickness
D_n	nominal outside diameter
$p_{d\text{-}apt}$	arbitrary-point-in-time pressure at the discharge end
$p_{s\text{-}apt}$	arbitrary-point-in-time pressure at the suction end
ρ	Pearson correlation coefficient
τ	Time lag in minute
$f_X(x)$	probability density function
$F_X(x)$	cumulative density function
$\xi, \lambda, \delta, \gamma$	Johnson SB distribution parameters
$p_{d\text{-}we}$	weekly maximum discharge pressures
$p_{d\text{-}me}$	monthly maximum discharge pressures
$p_{d\text{-}ae}$	annual maximum discharge pressures
$p_{s\text{-}we}$	weekly maximum suction pressures
$p_{s\text{-}me}$	monthly maximum suction pressures
$p_{s\text{-}ae}$	annual maximum suction pressures
α, β, a, b	Beta distribution parameters
τ_{0d}, τ_{0s}	Autocorrelation parameters
$S_X(f)$	PSD function
$S_{d\text{-}apt}(f)$	PSD function for arbitrary-point-in-time discharge pressure
$\rho_{d\text{-}apt}(\tau)$	Correlation for arbitrary-point-in-time discharge pressure
$\rho_{s\text{-}apt}(\tau)$	Correlation for arbitrary-point-in-time suction pressure
$w(t)$	Window function
$x_k(t)$	periodogram
T_s	length of segment
α_2, λ_m	bandwidth parameters

Δp_d Discharge pressure range

Δp_s Suction pressure range

η, θ Fréchet distribution parameters

Chapter 3

g limit state function

r burst capacity at the defect

p internal pressure

D pipe outside diameter

wt wall thickness

σ_u tensile strength of the pipe steel

ξ model error associated with the PCORROC model

d_{max} defect depth

l defect length

g_d depth growth rate per year

$P_{f,i}(t)$ instantaneous failure probability of the corrosion defect at year t

$\beta(t)$ reliability index

$P_f(t)$ failure probability of the corrosion defect up to year t since time zero

wt_n nominal pipe wall thickness

D_n nominal outside diameter

ξ, λ, $\delta\,\gamma$ Johnson SB distribution parameters

p_{d-we} weekly maximum discharge pressures

p_{d-me} monthly maximum discharge pressures

p_{d-ae} annual maximum discharge pressures

$S_d(f)$ single-sided PSD function of the discharge pressure

1 Introduction

1.1 Background

Pipeline system is one of the most efficient and safest transportation method that conveys crude oil and natural gas from the production sites to the next users comparing with other means of transporting method, for example, tanker trucks, rails (Green and Jackson, 2015). As the major operational load for the oil and gas pipeline, the internal pressure is generally qualified to be operated under the form of maximum operating pressure (MOP) and controlled based on a given standard, such as, the Canadian pipeline standard CSA Z662-19 (CSA 2019). Typically in fitness-for-service (FFS) assessment, MOP is chosen to compare with the remaining pressure containment capacity, i.e. burst capacity, of the pipeline after the in-service pipeline experienced flaws such as the corrosion defects and cracks. The actual internal pressure of an operating pipeline is, on the other hand, varying all the time, as a result, it should be viewed as a stochastic process instead of a deterministic value. The pressure fluctuation for crude oil pipeline is generally much higher than that in natural gas pipeline as the matter of significant difference in the compressibility of liquid and gas. (Zhang and Zhou 2015, Zhao 2016).

The reliability-based integrity management program offers a general framework to accounts for various uncertainties involved in the FFS assessment including the pipe material properties, defect sizes and internal pressure. According to the Pipeline and Hazardous Material Safety Administration (PHMSA) of the US Department of Transportation, corrosion is one of the most common causes of the pipeline incidents. (Lam and Zhou 2016). Reliability-based corrosion management program is being increasingly used to pipeline operators to assess the uncertainties associated with the pipe material properties, corrosion growth and the internal pressure

(Kariyawasam and Peterson 2010). High-resolution inline inspections (ILI) of the pipeline are carried out in a timely manner to capture the defect sizes of the corrosion on the pipeline. Then, the corrosion growth model is characterized based on the ILI data and corresponding reliability analyses is conducted to evaluate the failure probability of the pipeline. Finally, mitigation actions is taken according to the failure probability obtained in the previous step to make sure the program is under sound maintenance budget and manpower. (Gong and Zhou 2018). Different probabilistic properties of the internal pressure are chosen considering different threat or limit state in the reliability-based FFS assessment. A wide range of assumptions are given in the previous studies (Keshtegar et al.2019, Teixeira et al 2008, Ahammed and Melchers 1996). However, it is not clear if the statistics are obtained from actual pipeline since the sources are mostly not mentioned. Most of the studies also haven't state clearly if the pipeline is used for oil or gas transportation which we learn from above that the difference between make have a major impact on the pressure performance.

1.2 Objective and research significance

The objectives of this thesis include: 1) Characterize the statistics of the pressure record of a particular oil pipeline and investigate the probabilistic characteristics of the internal pressure. 2) Investigate the implications of probabilistic characteristics of the internal pressure reported in the internal pressure characteristics summarized for the reliability analysis of corroding pipelines.

1.3 Scope of the study

This thesis consists of two main topics which are presented in Chapters 2 and 3.

In Chapter 2, A Canadian pipeline company provided the present study with minute-by-minute pressure records collected over durations of at least one year from the discharge and suction ends of one pump station on a crude oil transmission pipeline owned and operated by the company.

Statistical analyses of these pressure records are carried out in the present study to investigate the probabilistic characteristics of the internal pressure. The analysis results shed light on how the internal pressure of crude oil transmission pipelines can be appropriately characterized in the reliability-based FFS assessment.

In Chapter 3, it is investigated the implications of probabilistic characteristics of the internal pressure reported in Chapter 2 for the reliability analysis of corroding pipelines. Two hypothetical crude oil pipeline examples are considered in the analysis. Both examples are assumed to have the same MOP as the real pipeline from which the pressure records are obtained. The probabilities of failure of representative corrosion defects are then evaluated based on ILI-reported defect sizes and corrosion growth rates that are commonly assumed in the literature (Zhou 2010). The pipeline internal pressure is considered as a random variable or stochastic process in the reliability analysis. The probabilistic characteristics of the internal pressure from this research as well as in the literature are considered in the reliability analysis, and the corresponding failure probabilities are compared to shed light on the impact of the internal pressure on the evaluated failure probability. The first-order and second-order reliability method (FORM and SORM) and simple Monte Carlo simulation (MCS) are employed to evaluate the failure probabilities of the corroding pipelines as a function of time.

1.4 Thesis format

This thesis is prepared in an Integrated-Article Format as specified by the School of Graduate and Postdoctoral Studies at Western University, London, Ontario, Canada. Seven chapters are included in the thesis. Chapter 1 presents the introduction of the thesis which includes the research background, objective and research significance, scope of the study and thesis format. Chapters 2 through 3 are the main body of the thesis, of which each chapter solves an individual topic. The

main conclusions and recommendations for future research regarding the topics in the thesis are provided in Chapter 4.

Reference

Ahammed M, Melchers RE. Reliability estimation of pressurised pipelines subject to localised corrosion defects. International Journal of Pressure Vessels and Piping. 1996 Dec 1;69(3):267-72.

Canadian Standard Association (CSA) Z662-15, Oil and gas pipeline system, Canadian Standard Association, Mississauga, ON, Canada. 2016

Gong C, Zhou W. Multi-objective maintenance strategy for in-service corroding pipelines using genetic algorithms. Structure and Infrastructure Engineering. 2018 Nov 2;14(11):1561-71.

Green, K. P., and Jackson, T. (2015). Safety in the transportation of Oil and Gas: pipelines or rail?. Vancouver, BC: Fraser Institute.

Kariyawasam S, Peterson W. Effective improvements to reliability based corrosion management. InInternational Pipeline Conference 2010 Jan 1 (Vol. 44236, pp. 603-615).

Keshtegar B, Seghier ME, Zhu SP, Abbassi R, Trung NT. Reliability analysis of corroded pipelines: novel adaptive conjugate first order reliability method. Journal of Loss Prevention in the Process Industries. 2019 Nov 1;62:103986.

Lam C, Zhou W. Statistical analyses of incidents on onshore gas transmission pipelines based on PHMSA database. International Journal of Pressure Vessels and Piping. 2016 Sep 1;145:29-40.

Teixeira AP, Soares CG, Netto TA, Estefen SF. Reliability of pipelines with corrosion defects. International Journal of Pressure Vessels and Piping. 2008 Apr 1;85(4):228-37.

Zhang S, Zhou W. Probabilistic characterisation of metal-loss corrosion growth on underground pipelines based on geometric Brownian motion process. Structure and Infrastructure Engineering. 2015 Feb 1;11(2):238-52.

Zhao J, Chevil K, Chen W, Been J, Keane S. Optimized Methods of Recording Pipeline Pressure Fluctuations for Pipeline Integrity Analysis. InInternational Pipeline Conference 2016 Sep 26 (Vol. 50251, p. V001T03A060). American Society of Mechanical Engineers.

Zhou W. System reliability of corroding pipelines. International Journal of Pressure Vessels and Piping. 2010 Oct 1;87(10):587-95.

2 Probabilistic characterization of internal pressure of crude oil transmission pipelines based on pressure records

2.1 Introduction

The internal pressure is the most important operational load for oil and gas pipelines. The maximum operating pressure (MOP) is the maximum pressure the pipeline is qualified to be operated according to a given standard, e.g. the Canadian pipeline standard CSA Z662-19 (CSA 2019). In deterministic fitness-for-service (FFS) assessment of in-service pipelines containing flaws such as corrosion defects and cracks, the remaining pressure containment capacity, i.e. burst capacity, of the pipeline is evaluated and compared with MOP multiplied by a factor of safety to determine if immediate rehabilitation actions for the pipeline are necessary (Kiefner and Vieth 1986). The actual internal pressure of an in-service pipeline is however uncertain and fluctuates with time; therefore, it is a stochastic process. Due to the significant difference in the compressibility of liquid and gas, the pressure fluctuation in liquid pipelines, e.g. crude oil pipelines, is generally much higher than that in gas pipelines (Zhang and Zhou 2015).

The reliability-based pipeline integrity management program (Nessim et al. 2004; Kariyawasam and Huyse 2012) is being increasingly adopted by the pipeline industry as it provides a consistent framework to accounts for various uncertainties involved in the FFS assessment, e.g. pipe geometric and material properties, sizes of flaws and the internal pressure. The probabilistic characteristics of the internal pressure considered in the reliability-based FFS assessment depend on the nature of the integrity threat (i.e. limit state). For example, probabilistic characteristics of the arbitrary-point-in-time internal pressure are relevant to the immediate failure (burst) of a dent-gouge caused by an excavating equipment accidentally impacting the pipeline (Nessim and Zhou 2005). This is because equipment impact on pipelines generally happens randomly in time. A

dent-gouge that does not fail immediately at the time of impact may fail later (i.e. delayed failure) (Kiefner et al. 2001; Nessim and Zhou 2005) as a result of the internal pressure reaching a peak value and/or growth of the gouge due to fatigue. In this case, probabilistic characteristics of the maximum internal pressure over a reference period of time are relevant to the delayed dent-gouge failure. The same characteristics are also relevant to the burst limit state of a pipeline at a corrosion or stress corrosion cracking (SCC) defect. This is because corrosion and SCC generally grow slowly over time; therefore, the remaining burst capacity of the pipeline containing the corrosion or SCC defect deteriorates slowly. It follows that burst failure at a corrosion or SCC defect is more likely to occur when the internal pressure of the pipeline is at peak values over a reference time period. Pipelines containing such flaws as seam weld cracks and dents may fail by fatigue due to the cyclic nature of the internal pressure (Nessim and Zhou 2005; Alexander and Kiefner 1999). In this case, probabilistic characteristics of the pressure range obtained from a suitable cycle counting method (e.g. the rainflow counting) are relevant to the corresponding fatigue limit states.

Probabilistic characteristics of the pipeline internal pressure have been suggested in the literature and pipeline standards. For natural gas pipelines operating at capacity, the Canadian pipeline standard, CSA Z662-19 suggests that the ratio between the annual maximum internal pressure (p_{ae}) and MOP can be characterized by a beta distribution with a mean of 0.993, a coefficient of variation (COV) of 3.4%, a lower bound of 80% and an upper bound of 110% based on the pressure record from one pipeline operator, and a beta distribution with a mean of 0.865, a COV of 8.4%, and lower and upper bounds equal to 60% and 110%, respectively, is suggested for the ratio between the arbitrary-point-in-time pressure and MOP. Jiao et al. (1995) suggested that p_{ae}/MOP follow a Gumbel distribution a mean between 1.03 and 1.07 and a COV between 1 and 2%. Statistics of the internal pressure in oil pipelines or other types of liquid pipelines are however not

provided in CSA Z662-19. The internal pressure is typically assumed to be a random variable (as opposed to a stochastic process) in reliability analyses of corroded pipelines reported in the literature. For example, Ahammed and Melchers (1996) assumed the internal pressure to follow a normal distribution with a COV of 5%; Teixeira et al. (2008) assumed the internal pressure to follow a Gumbel distribution with a mean equal to 0.97MOP and a COV of 7%, and Keshtegar et al. (2019) assumed the internal pressure to follow a normal distribution with a COV of 10%. The bases for the above-indicated statistics are not provided; furthermore, it is unclear if the statistics apply to the internal pressure of gas or liquid pipelines. Zhang and Tian (2020) assumed a Gumbel distribution with a COV of 8% for the internal pressure without providing the basis for the assumption. Zhou (2010) considered the internal pressure as a stochastic process in the reliability analysis of corroding pipelines and simplified the pressure as a discrete Ferry-Borges process consisting of a sequence of independent and identically distributed (IID) random variables, each representing the annual maximum internal pressure. Zhang and Zhou (2013) characterized the internal pressure as a Poisson square wave process in the reliability analysis of corroding pipelines. However, both the Ferry-Borges and Poisson square wave processes are assumed primarily to facilitate the reliability analysis; the validity of these assumptions has yet to be confirmed based on internal pressure records collected from actual in-service pipelines.

A Canadian pipeline company provided the present study with minute-by-minute pressure records collected over durations of at least one year from the discharge and suction ends of one pump station on a crude oil transmission pipeline owned and operated by the company. Statistical analyses of these pressure records are carried out in the present study to investigate the probabilistic characteristics of the internal pressure. The analysis results shed light on how the internal pressure of crude oil transmission pipelines can be appropriately characterized in the

reliability-based FFS assessment. The rest of this paper is organized as follows. Section 2 presents details of the pressure records and the basic information of the pipeline from which the pressure records were collected. Section 3 describes statistics of the arbitrary-point-in-time pressure as well as weekly, monthly and annual maximum pressures obtained from the pressure records. Key characteristics of the internal pressure as a stochastic process such as the correlation length and power spectral density (PSD) function are also evaluated from the pressure records and presented in Section 3. Section 4 describes the statistics of the pressure ranges obtained from the rainflow counting of the pressure records, followed by conclusions in Section 5.

2.2 Details of Pressure Records

Pump stations are typically built at strategically selected locations along the route of a long transmission pipeline to ensure the proper pressurization of the pipeline and consistent flow of the hydrocarbon product being transported. The product is compressed to the desired pressure level in the pump station before being released at the discharge end of the station. As the product is transported along the pipeline, the pressure gradually drops until the product reaches the suction end of the next pump station for compression again. It follows that the characteristics of pressures at the discharge and suction ends of the pump station are different. The crude oil transmission pipeline for which the pressure records were provided to the present study has an MOP of 9.9 MPa with a design factor (FS) of 0.80. The nominal pipe wall thickness (t_n) and outside diameter (D_n), specified minimum yield strength (SMYS) of the pipe steel, and MOP are related through the well-known Barlow equation as follows (CSA 2019):

$$t_n = \frac{D_n \cdot MOP}{2 \cdot FS \cdot SMYS} \tag{2.1}$$

For confidentiality reasons, the values of D_n, t_n and SMYS of the pipeline are not disclosed in this study. The minute-by-minute pressure records at the discharge and suction ends of a pump station on the pipeline are depicted in Fig. 2.1. The duration of the discharge pressure record is 1.5 years, whereas the duration of the suction pressure record is 1.0 year. A distinct upper bound of the discharge pressure equal to approximately 90%MOP can be observed from Fig. 2.1, which suggests that the pipeline is operating at 90% of its full capacity. The suction pressure has a distinct lower bound of about 4%MOP. Figure 2.1 further suggests that the suction end appears to experience more pressure cycles per unit time than the discharge end.
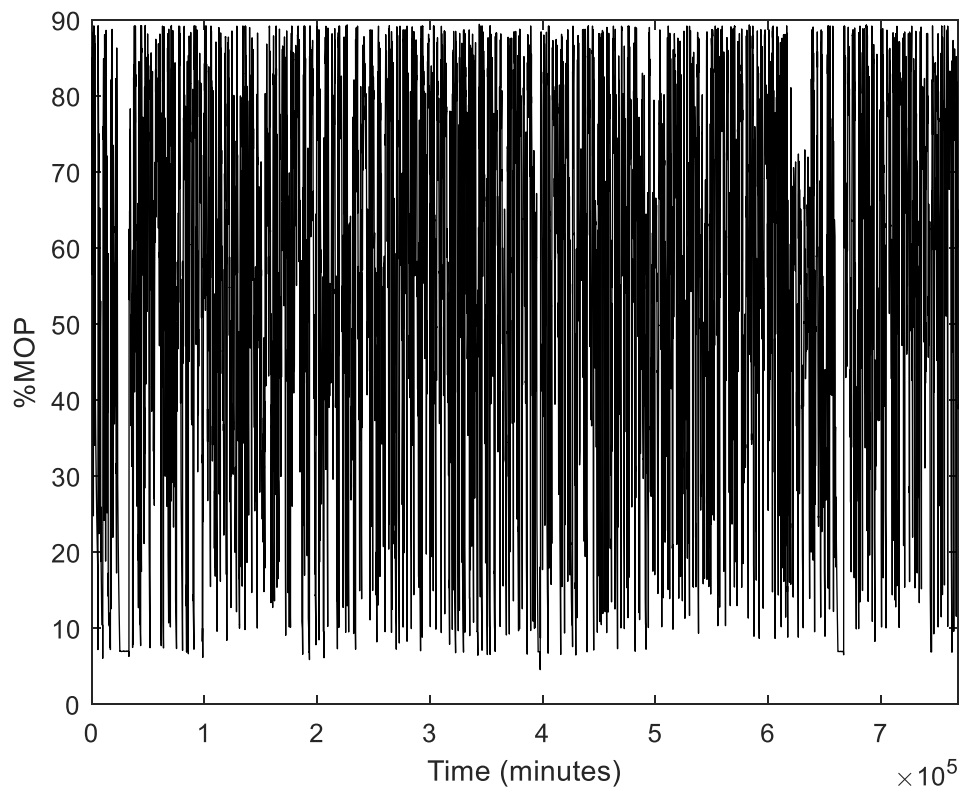
(a) Discharge pressure
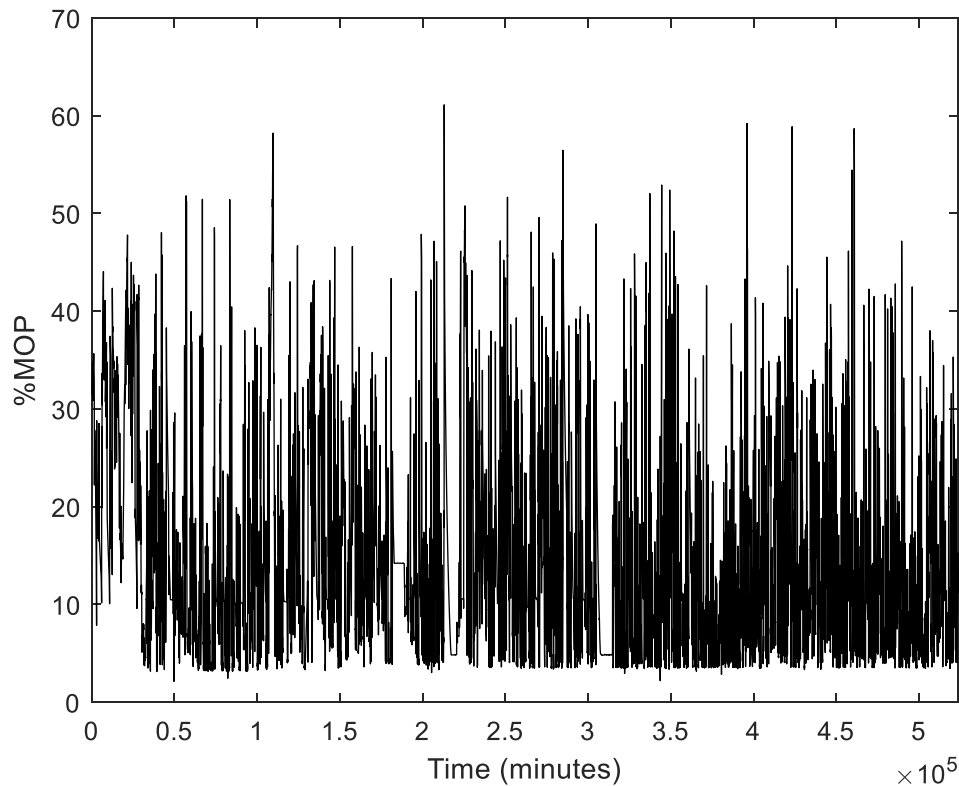
(b) Suction pressure

Fig. 2.1 Minute-by-minute pressure records at the discharge and suction ends of a pump station on a crude oil transmission pipeline

2.3 Statistics of arbitrary-point-in-time and extreme pressures

2.3.1 Arbitrary-point-in-time pressures

Let $p_{d\text{-}apt}$ and $p_{s\text{-}apt}$ denote, respectively, the arbitrary-point-in-time pressures at the discharge and suction end of the pump station. To derive the statistics of $p_{d\text{-}apt}$ and $p_{s\text{-}apt}$, well-separated data points from the discharge and suction pressure records need to be collected such that these data points are approximately considered independent and identical distributed. To this end, the Pearson correlation coefficient (ρ) between two sets of data points on the pressure record separated

by a given time lag τ (min) is evaluated. Table 2.1 summarizes values of ρ corresponding to different values of τ for the discharge and suction pressures.

Table 2.1 Pearson correlation coefficients for discharge and suction pressures separated by different time lags

Time lag τ (minutes)	ρ	
	Discharge pressure	Suction pressure
50	0.89	0.85
100	0.80	0.78
200	0.63	0.68
400	0.40	0.56
800	0.16	0.41
1000	0.10	0.36
3000	0.001	0.14

Table 2.1 indicates that as τ increases the correlation coefficient of the discharge pressures decreases more rapidly than that of the suction pressures. Discharge pressures separated by $\tau \geq$ 1000 minutes can be considered uncorrelated, whereas suction pressures with $\tau \geq 3000$ minutes can be considered uncorrelated. Subsequently, 768 discharge pressures with $\tau = 1000$ min. and 174 suction pressures with $\tau = 3000$ min. are selected from the pressure records and employed to evaluate the statistics of $p_{d\text{-}apt}$ and $p_{s\text{-}apt}$ (Table 2.2). The empirical cumulative distribution functions (CDF) of $p_{d\text{-}apt}$ and $p_{s\text{-}apt}$ are depicted in Fig. 2.2. Distribution fitting techniques are then employed to find the best-fit probability distributions to characterize $p_{d\text{-}apt}$ and $p_{s\text{-}apt}$ using the commercial software, EasyFit (Version 5.6 [e]MathWave Technologies). It is observed that the Johnson SB (JSB) distribution (Johnson 1949) fits samples of $p_{d\text{-}apt}$ and $p_{s\text{-}apt}$ well. The probability density function (PDF) and CDF, $f_X(x)$ and $F_X(x)$, of a random variable X that follows a JSB distribution are given by:

$$f_X(x) = \frac{\delta}{\lambda\sqrt{2\pi}z(1-z)} exp\left(-\frac{1}{2}\left(\gamma + \delta\,ln\left(\frac{z}{1-z}\right)\right)^2\right) \tag{2.2}$$

$$F_X(x) = \Phi\left(\gamma + \delta\,ln\left(\frac{z}{1-z}\right)\right) \tag{2.3}$$

where $z = \frac{x-\xi}{\lambda}$; x denotes the value of X; ξ, λ, δ and γ are distribution parameters, and $\Phi(\bullet)$ denotes

the CDF of the standard normal distribution. Note that JSB is a bounded distribution with the

lower and upper bounds equal to ξ and $\xi + \lambda$, respectively. Based on Fig. 2.1, the lower and upper

bounds of $p_{d\text{-}apt}$ are set to zero and 0.9MOP, respectively, i.e. $\xi = 0$ and $\lambda = 0.9$MOP, whereas the

lower and upper bounds of $p_{s\text{-}apt}$ are set to zero and 0.7MOP, respectively, i.e. $\xi = 0$ and $\lambda =$

0.7MOP. The values of ξ, λ, δ and γ corresponding to $p_{d\text{-}apt}$ and $p_{s\text{-}apt}$ are summarized in Table 2.2,

whereby δ and γ are obtained from the maximum likelihood estimation. The JSB CDFs are

depicted in Fig. 2.2 for comparison with the empirical CDFs. Table 2.2 indicates that the suction

pressure is on average substantially lower than the discharge pressure, although the former has

greater variability than the latter.

Table 2.2 Summary of statistics of $p_{d\text{-}apt}$ and $p_{s\text{-}apt}$

	$p_{d\text{-}apt}$	$p_{s\text{-}apt}$
Number of samples	768	174
Sample mean (%MOP)	57.3	13.8
Sample COV (%)	41.0	71.9
Sample min (%MOP)	6.9	3.4
Sample max (%MOP)	89.2	45.5
ξ (%MOP)	0	0
λ (%MOP)	90	70
δ	0.69	1.88
γ	-0.53	1.17
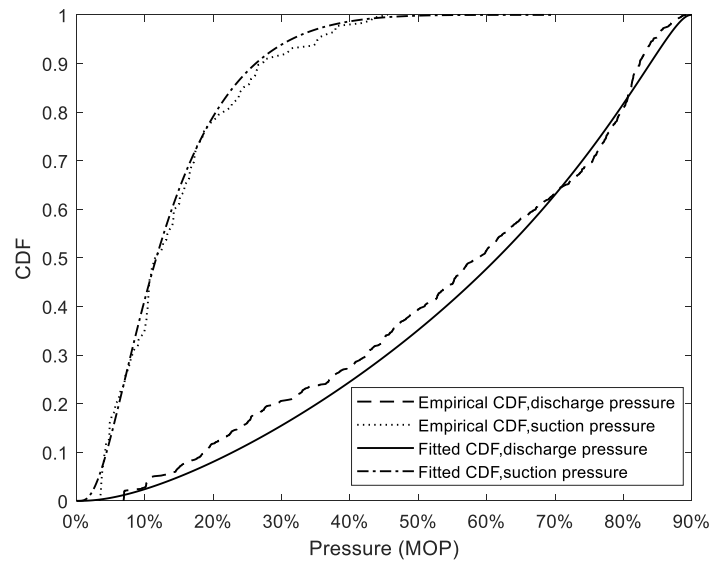
Fig. 2.2 Empirical and fitted CDFs of arbitrary point-in-time discharge and suction pressures

2.3.2 Extreme pressures

As described in the Introduction section, the maximum pressure over a reference period is relevant to the reliability analysis of pipelines subjected to slowly degradation mechanisms. Therefore, probabilistic characteristics of the extreme pressures are derived based on the corresponding samples (Fig. 2.3) collected from the pressure records provided. Let $p_{d\text{-}we}$, $p_{d\text{-}me}$ and $p_{d\text{-}ae}$ denote the weekly, monthly and annual maximum discharge pressures, respectively, and $p_{s\text{-}we}$, $p_{s\text{-}me}$ and $p_{s\text{-}ae}$ denote the weekly, monthly and annual maximum suction pressures, respectively. The statistics of $p_{d\text{-}we}$, $p_{d\text{-}me}$, $p_{s\text{-}we}$ and $p_{s\text{-}me}$ evaluated from the corresponding samples are summarized in Table 2.3.

Table 2.3 Summary of sample statistics of weekly and monthly maximum discharge and suction pressures

	$p_{d\text{-}we}$	$p_{d\text{-}me}$	$p_{s\text{-}we}$	$p_{s\text{-}me}$
Number of samples	76	18	52	12
Sample mean (%MOP)	88.7	89.3	45.7	53.7
Sample COV (%)	2.3	0.07	27.7	9.3

Sample min (%MOP)	72.9	89.2	22.6	46.6
Sample max (%MOP)	89.4	89.4	61.1	61.1

(a) $p_{d\text{-}we}$ and $p_{s\text{-}we}$

(b) $p_{d\text{-}me}$ and $p_{s\text{-}me}$

Fig. 2.3 Weekly and monthly maximum discharge and suction pressure time series

Figure 2.3 indicates that $p_{d\text{-}we}$ and $p_{d\text{-}me}$ have small variability; in fact, the results in Table 3 indicate that the variability of $p_{d\text{-}me}$ is negligibly small. It follows that $p_{d\text{-}me}$ can be assumed to be a deterministic qua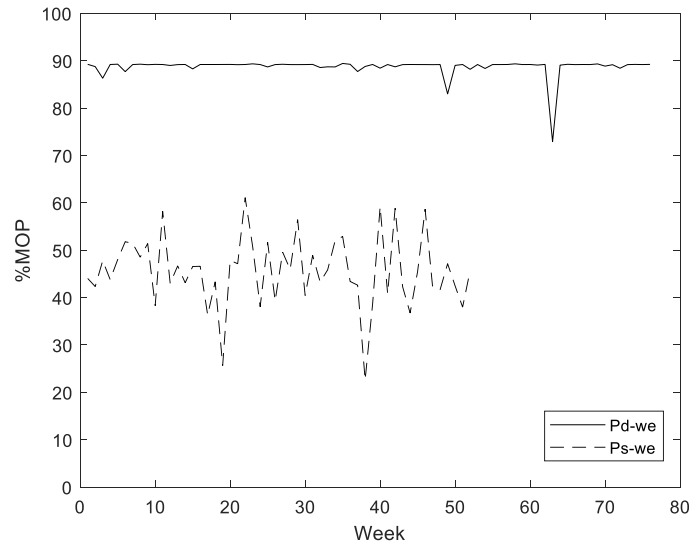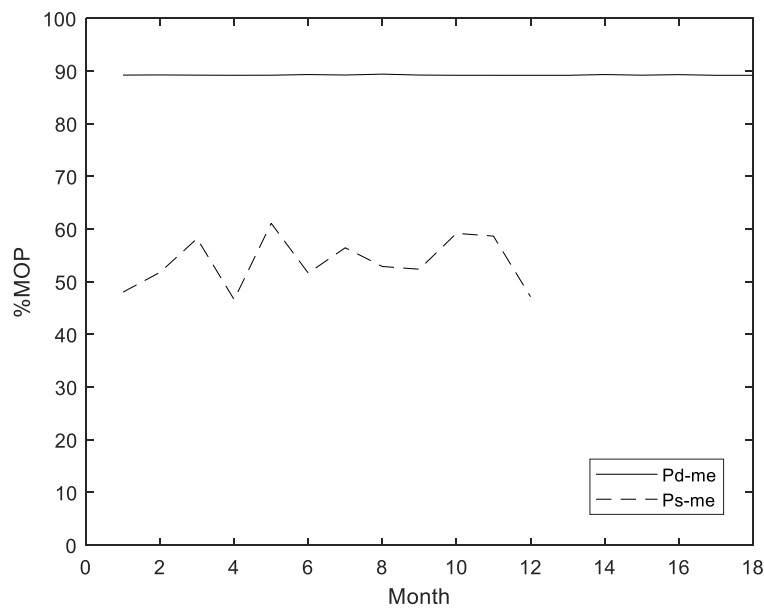ntity equal to 0.9MOP, i.e. the capacity at which the pipeline is operating. This further suggests that $p_{d\text{-}ae}$ can be assumed to be a deterministic quantity that equals 0.9MOP. This observation differs markedly from the annual maximum pressure distributions commonly suggested in the literature. It may be further inferred that $p_{d\text{-}me}$ and $p_{d\text{-}ae}$ could be assumed to equal MOP had the pipeline been operating at its full capacity as opposed to 90% capacity. This assumption of course needs to be confirmed with the corresponding pressure data in future studies. The variability of $p_{d\text{-}we}$ is also small (sample COV equal to 2.3%); furthermore, this variability is due largely to a marked drop in the maximum weekly pressure in week 63 (see Fig. 3(a)). If this data point is excluded, the sample COV of $p_{d\text{-}we}$ decreases to less than 1%. This suggests that $p_{d\text{-}we}$ can also be considered a deterministic quantity equal to 0.9MOP.

In contrast to the extreme discharge pressures, the variability of the weekly and monthly maximum suction pressure is relatively high. The beta distribution is found to fit samples of the weekly and monthly maximum suction pressures. The PDF of a beta distributed random variable Y, $f_Y(y)$, is given by,

$$f_Y(y) = \frac{1}{B(\alpha,\beta)} \frac{(y-a)^{\alpha-1}(b-y)^{\beta-1}}{(b-a)^{\alpha+\beta-1}} \tag{2.4}$$

where a and b are the lower and upper bounds of the beta distribution, respectively; α and β are the distribution parameters, and $B(\alpha, \beta) = \Gamma(\alpha)\Gamma(\beta)/\Gamma(\alpha + \beta)$ with $\Gamma(\bullet)$ being the gamma function.

The mean and COV of Y equal $(a + (b-a)\alpha/(\alpha + \beta))$ and $\dfrac{\sqrt{\frac{\alpha\beta}{\alpha+\beta+1}}}{\alpha+\frac{a(\alpha+\beta)}{(b-a)}}$, respectively. By setting $a = 0$ and $b = 0.7$MOP for both $p_{s\text{-}we}$ and $p_{s\text{-}me}$, the values of α and β for $p_{s\text{-}we}$ and $p_{s\text{-}me}$ are evaluated

using the maximum likelihood method and summarized in Table 4. Since the duration of the suction pressure record is one year, it is not feasible to derive the probability distribution of $p_{s\text{-}ae}$ from samples. Therefore, the extreme value analysis is carried out to derive the probability distribution of $p_{s\text{-}ae}$ from that of $p_{s\text{-}me}$. The probability of $p_{s\text{-}ae}$ less than or equal to a given pressure p, $Prob(p_{s\text{-}ae} \leq p)$, can be evaluated from the probability of $p_{s\text{-}me} \leq p$, $Prob(p_{s\text{-}me} \leq p)$, as follows:

$$P(p_{s-ae} \leq p) = \left(P(p_{s-me} \leq p)\right)^{12} \tag{2.5}$$

By selecting a series of p values between 0.5MOP and 0.7MOP, the corresponding CDF values of $p_{s\text{-}ae}$ are obtained from Eq. (2.5). Note that $Prob(p_{s\text{-}me} \leq p)$ is evaluated using the fitted beta distribution as indicated in Table 2.4. The beta distribution with $a = 0$ and $b = 0.7$MOP is again selected to fit CDF values of $p_{s\text{-}ae}$ obtained from the extreme value analysis, with the corresponding values of α and β summarized in Table 2.4. The fitted beta distributions of $p_{s\text{-}we}$, $p_{s\text{-}me}$ and $p_{s\text{-}ae}$ are depicted in Fig. 2.5, along with the corresponding empirical CDFs from the samples or extreme value analysis.

Table 2.4 Parameters of fitted beta distributions for $p_{s\text{-}we}$ and $p_{s\text{-}me}$

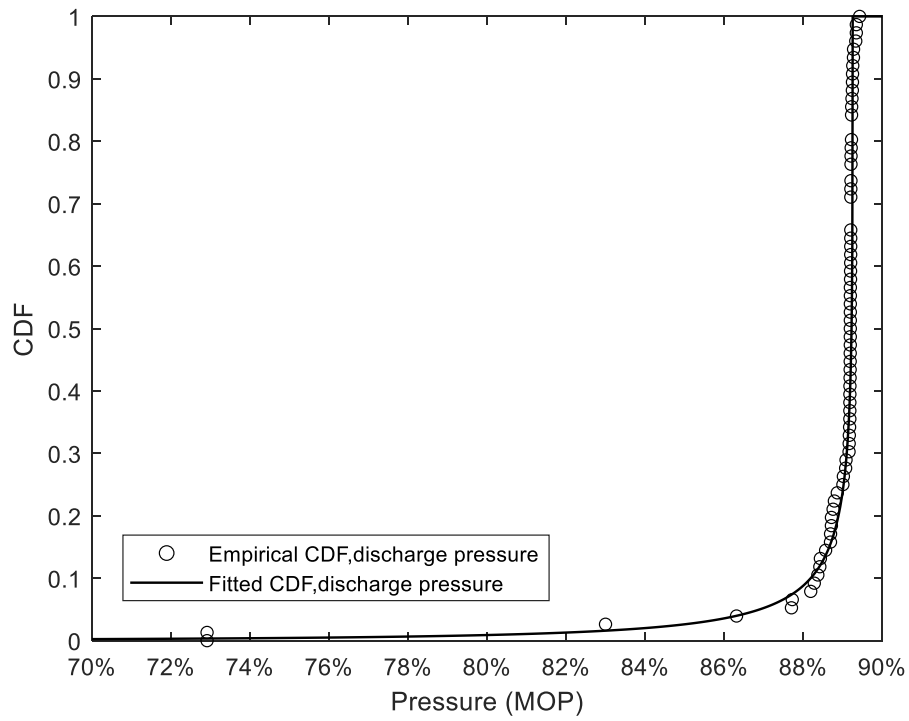| Parameters of beta distribution	$p_{s\text{-}we}$	$p_{s\text{-}me}$	$p_{s\text{-}ae}$
α	11.94	15.23	169.27
β	6.36	4.74	23.28
a (%MOP)	0	0	0
b (%MOP)	70	70	70

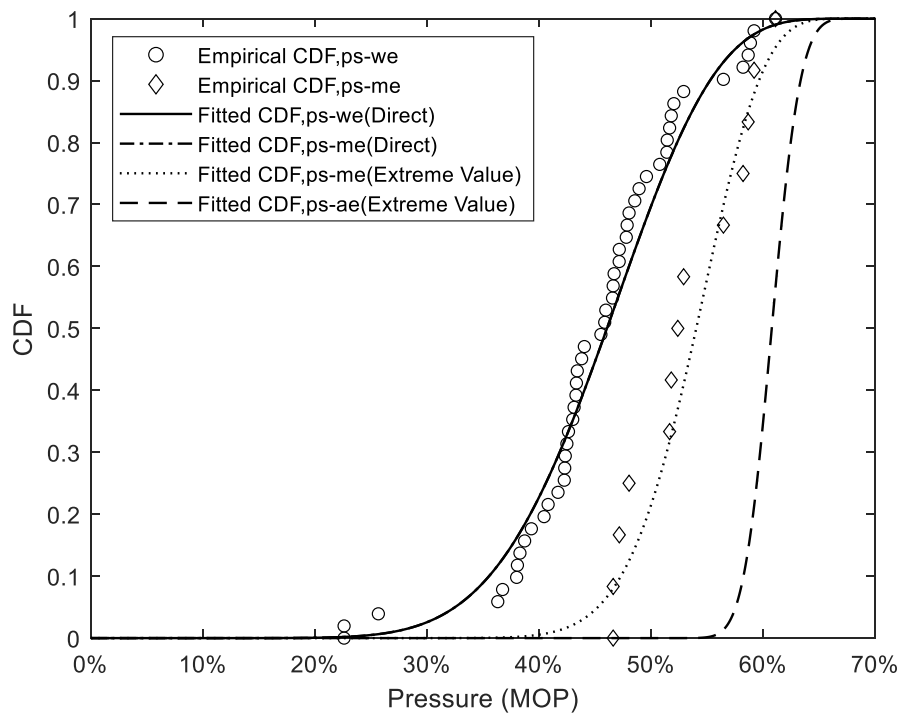Fig 2.4. Fitted CDF of weekly maximum of discharge pressure

Fig.2.5. Fitted and empirical CDFs of weekly, monthly and annual maximum suction pressures

2.4 Characteristics of the Discharge and Suction Pressures as Stochastic Processes

It is assumed that $p_{d\text{-}apt}$ and $p_{s\text{-}apt}$ are stationary stochastic processes. Key probabilistic characteristics of a stationary stochastic process include its marginal distribution function and its second-order properties, i.e. the autocorrelation function in the time domain and equivalently the power spectral density (PSD) function in the frequency domain (Vanmarcke 2010). Rosenfeld et al. (2002) pointed out that pipeline operators can identify operational events resulting in pressure cycles with implications for fatigue damage based on the frequency of events having prominent power peaks. The operator can then evaluate if the operation can be modified to reduce the frequency of occurrence of such events or eliminate them all together.

The marginal distributions of $p_{d\text{-}apt}$ and $p_{s\text{-}apt}$ have been discussed in Section 2.3. The autocorrelation function, $\rho_X(\tau)$, of a zero-mean stationary stochastic process $X(t)$ indexed by time (t) is defined as,

$$\rho_X(\tau) = \frac{E[(X(t)X(t+\tau)]}{\sigma_X^2} \tag{2.6}$$

where $E[\bullet]$ denotes expectation, and σ_X denotes the standard deviation of $X(t)$, respectively. Note that the mean and standard deviation of a stationary stochastic process are independent of time. It follows that $\rho_X(\tau) = 1$ for $\tau = 0$. As $\tau \to \infty$, it is expected that $X(t)$ and $X(t + \tau)$ are uncorrelated, which means $\rho_X(\tau) \to 0$ as $\tau \to \infty$. A stationary process with a non-zero mean can be converted to a zero-mean process by simply subtracting the mean value from the original process.

Table 2.1 summarizes the correlation coefficients between $p_{d\text{-}apt}$ ($p_{s\text{-}apt}$) separated by various values of the time lag τ. The exponential and γ-exponential correlation functions (Quinonero-Candela J, Rasmussen and Williams 2006) are found to fit the correlation coefficients well for the discharge and suction pressures, respectively.

$$\rho_{d-apt}(\tau) = \exp\left(-\frac{\tau}{\tau_{0d}}\right) \tag{2.7}$$

$$\rho_{s-apt}(\tau) = \exp\left(-\left(\frac{\tau}{\tau_{0s}}\right)^{\gamma}\right) \tag{2.8}$$

where $\rho_{d-apt}(\tau)$ and $\rho_{s-apt}(\tau)$ denote the autocorrelation functions for p_{d-apt} and p_{s-apt}, respectively; τ_{0d} and τ_{0s} are the so-called correlation lengths for p_{d-apt} and p_{s-apt}, respectively, and γ is the additional parameter in the γ-exponential function. The values of τ_{0d}, τ_{0s} and γ are evaluated to be 439 minutes (7.3 hrs), 966 minutes (16.1 hrs) and 0.60, respectively, from the curve fitting. It follows that two discharge (suction) pressures separated by more than 439 (966) minutes can be considered approximately uncorrelated. The fitted autocorrelation functions are depicted in Fig. 5 along with the correlation coefficients evaluated from the pressure records.
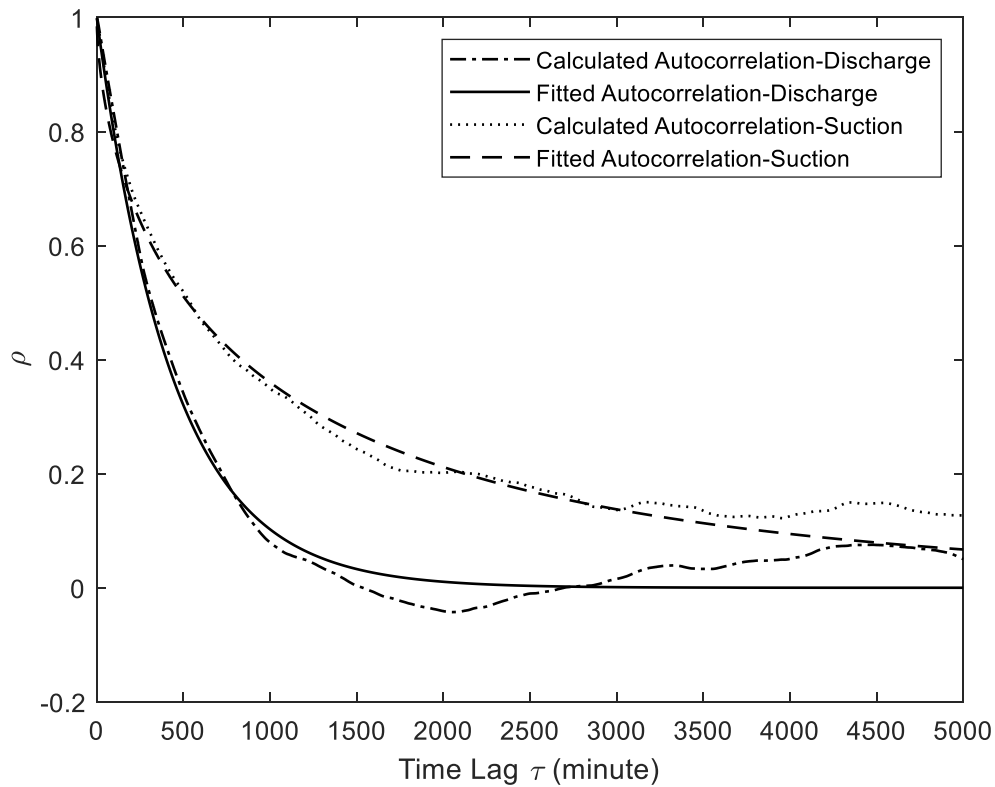

Fig. 2.6 Autocorrelation of arbitrary point-in-time discharge pressure

Let $S_X(f)$ denote the one-sided PSD function of $X(t)$, where f ($f > 0$) denotes the frequency in Hz. $S_X(f)$ is related to $\rho_X(\tau)$ through the celebrated Wiener-Khintchine relations (Vanmarcke 2010) as follows:

$$\frac{S_X(f)}{\sigma^2} = 4 \int_0^\infty \rho_X(\tau) \cos(2\pi f \tau) d\tau \tag{2.9}$$

$$\sigma^2 \rho_X(\tau) = \int_0^\infty S_X(f) \cos(2\pi f \tau) df \tag{2.10}$$

If $\rho_X(\tau)$ is the exponential correlation function, then the analytical expression of the corresponding $S_X(f)$ can be derived (Vanmarcke 2010). It follows that the PSD function of $p_{d\text{-}apt}$, $S_{d\text{-}apt}(f)$, corresponding to the exponential correlation function $\rho_{d\text{-}apt}(\tau)$ (i.e. Eq. (2.11)) is given by,

$$S_{d-apt}(f) = \frac{4(\sigma_{d-apt})^2 \tau_{0d}}{(2\pi f \tau_{0d})^2 + 1} \tag{2.11}$$

where $\sigma_{d\text{-}apt}$ is the standard deviation of $p_{d\text{-}apt}$. Equation (2.11) is consistent with the findings of Rosenfeld et al. (2020), who evaluated PSD functions of pressures in four different pipelines transporting natural gas, high vapour pressure liquid, crude oil and gasoline, respectively, and found that all four PSD functions are approximately proportional to $1/f^2$. There is no analytical expression of the PSD function of $p_{s\text{-}apt}$, $S_{s\text{-}apt}(f)$, corresponding to the γ-exponential correlation function $\rho_{s\text{-}apt}(\tau)$; therefore, $S_{s\text{-}apt}(f)$ can be evaluated from $\rho_{s\text{-}apt}(\tau)$ by carrying out the integral in Eq. (2.9) numerically. However, it is more efficient and accurate to evaluate the PSD function directly from sample records of the stochastic process (i.e. the pressure record in the present study) by utilizing the fast Fourier transform (FFT) algorithm (Bendat and Piersol 2010).

If an ensemble of records of $X(t)$, $x_k(t)$ ($0 \leq t \leq T$) ($k = 1, 2, \ldots$), is available, then $S_X(f)$ can be estimated as follows:

$$S_X(f) = \frac{2}{T} E[|X_k(f, T)|^2] \tag{2.12}$$

$$X_k(f,T) = \int_0^T x_k(t)e^{-i2\pi ft}dt \tag{2.13}$$

where T is the length of the record; $X_k(f, T)$ is the Fourier transform of $x_k(t)$ and can be efficiently computed numerically using the FFT; $|X_k(f, T)|^2 = X_k(f, T)X_k^*(f, T)$ with $X_k^*(f, T)$ being the complex conjugate of $X_k(f, T)$, and the expectation operation in Eq. (2.12) is with respect to all the records in the ensemble.

Welch's method (Solomon 1991) is used to numerically estimate PSD functions of $p_{d\text{-}apt}$ and $p_{s\text{-}apt}$ in this study. Welch's method estimates the PSD function from a single zero-mean time series record by partitioning the record into K overlapped segments (i.e. periodograms), $x_k(t)$ ($0 \le t \le T_s$) ($k = 1, 2, \ldots, K$), where T_s is the length of each segment. A windowed finite Fourier transform of each segment is then carried out as follows:

$$X_{kw}(f, T_s) = \int_0^{T_s} x_k(t)w(t)e^{-i2\pi ft}dt \tag{2.14}$$

where $w(t)$ is the window function. Commonly used window functions include the rectangular, Hanning, Hamming and Blackman (Solomon 1991). The numerical evaluation of the integral in Eq. (2.14) can be carried out efficiently using the FFT. Then $S_X(f)$ is estimated as,

$$S_X(f) = \frac{1}{K}\sum_{k=1}^{K}\frac{2}{WT_s}|X_{kw}(f, T_s)|^2 \tag{2.15}$$

$$W = \frac{1}{T_s}\int_0^{T_s}(w(t))^2 dt \tag{2.16}$$

In this study, each of the discharge and suction pressure records is partitioned into 3-month long segments. The overlap between consecutive segments is selected to be 50%. Consequently, there are 11 segments for the discharge pressure record and 7 segments for the suction pressure record, i.e. $K = 11$ (discharge pressure) or 7 (suction pressure). The rectangular window, i.e. $w(t) = 1$ for ($0 \le t \le T_s$), is employed. To facilitate the FFT analysis, each segment is zero padded at the end to

ensure the length of the segment to equal the nearest power of two that is longer than the original segment length. The PSD functions, $S_{d\text{-}apt}(f)$ and $S_{s\text{-}apt}(f)$, evaluated using Welch's method are depicted in Fig. 2.7, together with the analytical expression (i.e. Eq. (2.11)) for $S_{d\text{-}apt}(f)$. Since the sampling frequency of the pressure record is one minute, it follows that the Nyquist frequency (Bendat and Piersol 2010) for the spectral analysis equals 8.3×10^{-3} Hz, which is the highest frequency considered in the PSD functions evaluated using Welch's method. Figure 2.7 indicates that $S_{d\text{-}apt}(f)$ obtained from Welch's method agrees very well with Eq. (2.11). The figure also indicates that the dominant frequencies for both $S_{d\text{-}apt}(f)$ and $S_{s\text{-}apt}(f)$ are those below about 5.0×10^{-6} Hz, corresponding to pressure events with periods longer than 56 hours.
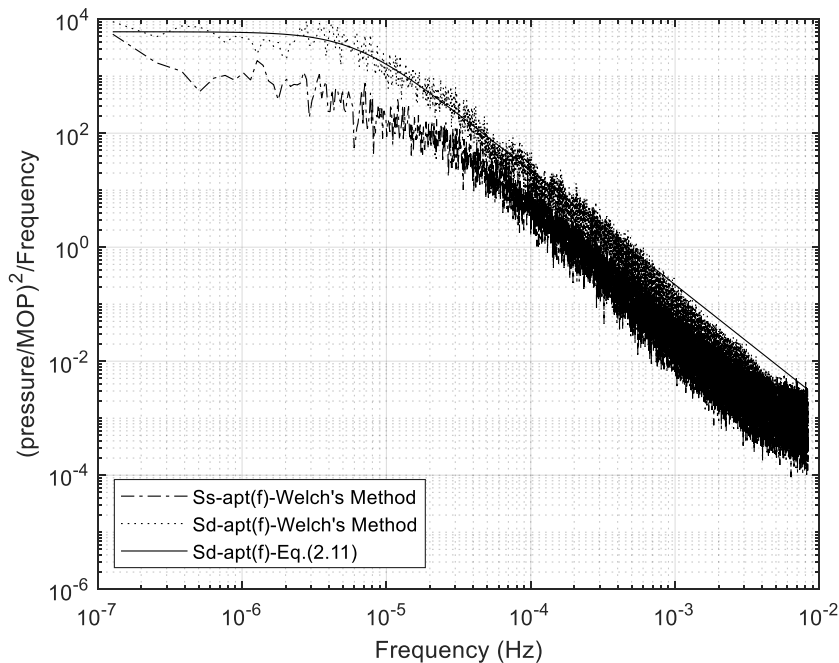

Fig. 2.7 PSD functions of discharge and suction pressures

Given the PSD function of $X(t)$, the bandwidth parameter, α_2 ($0 \leq \alpha_2 \leq 1$), of $X(t)$ (Bendat and Piersol 2010) can be evaluated as

$$\alpha_2 = \frac{\lambda_2}{\sqrt{\lambda_0 \lambda_4}} \tag{2.17}$$

$$\lambda_m = \int_0^\infty f^m S_X(f)df \ (m = 2, 4) \tag{2.18}$$

The process $X(t)$ is wide-banded if α_2 is close to zero and narrow-banded if α_2 is close to unity. The values of α_2 of the discharge and suction pressures are calculated to be 0.023 and 0.010 respectively, based on the corresponding PSD functions. It follows that both pressures are considered wide-band processes.

2.5 Probabilistic characteristics of pressure ranges

The rain flow counting analysis (ASTM 2017) is applied to the discharge and suction pressure records to evaluate the corresponding pressure ranges Δp_d and Δp_s. It is observed that both pressure records contain a large number of small pressure ranges; those pressure ranges less than or equal to 0.1%MOP are considered to have a negligible contribution to the fatigue damage due to pressure cycles and therefore ignored. By considering pressure ranges that are greater than 0.1%MOP, the statistics of Δp_d and Δp_s are summarized in Table 2.5. The histograms of Δp_d and Δp_s are depicted in Fig. 2.8. The Fréchet distributions are found to fit the data of Δp_d and Δp_s reasonably well. The PDF of a Fréchet distributed random variable Z, $f_Z(z)$, is given by,

$$f_Z(z) = \frac{\eta}{\theta}\left(\frac{\theta}{z}\right)^{\eta+1} \exp\left(-\left(\frac{\theta}{z}\right)^{\eta}\right) \tag{2.19}$$

where η and θ are the shape and scale parameters, respectively. The fitted and empirical CDF of Δp_d and Δp_s are depicted in Fig. 2.9, with the shape and scale parameters of the fitted CDF summarized in Table 2.5.

Table 2.5 Summary of statistics of Δp_d and Δp_s

Statistics	Δp_d	Δp_s
# of cycles per year	20625	26992
Mean (%MOP)	2.03	1.17
COV	3.39	3.52

Minimum (%MOP)	0.1	0.1
Maximum (%MOP)	84.61	59.10
η	0.93	1.08
θ	0.25	0.20

(a) Δp_d
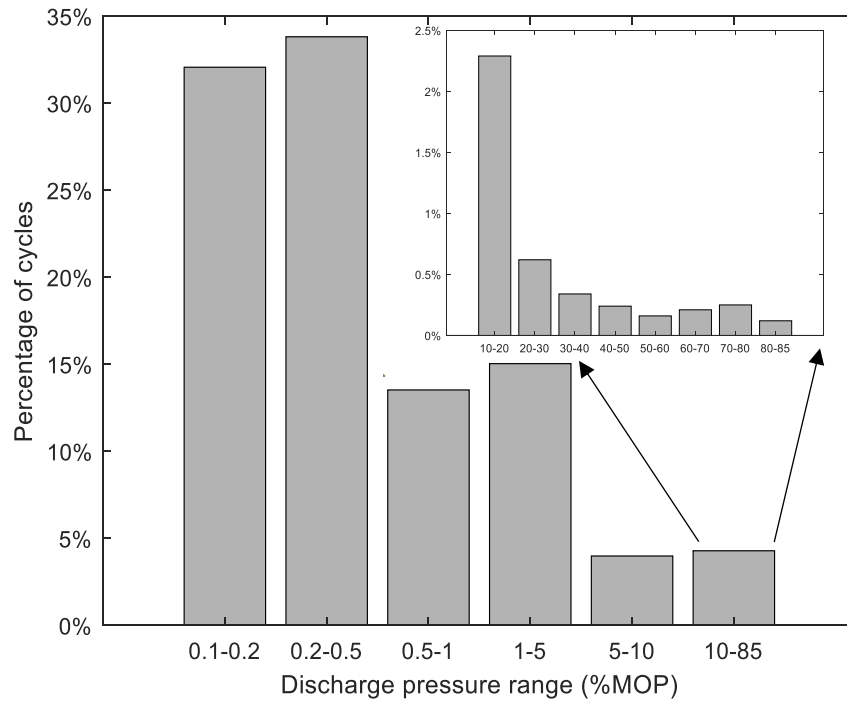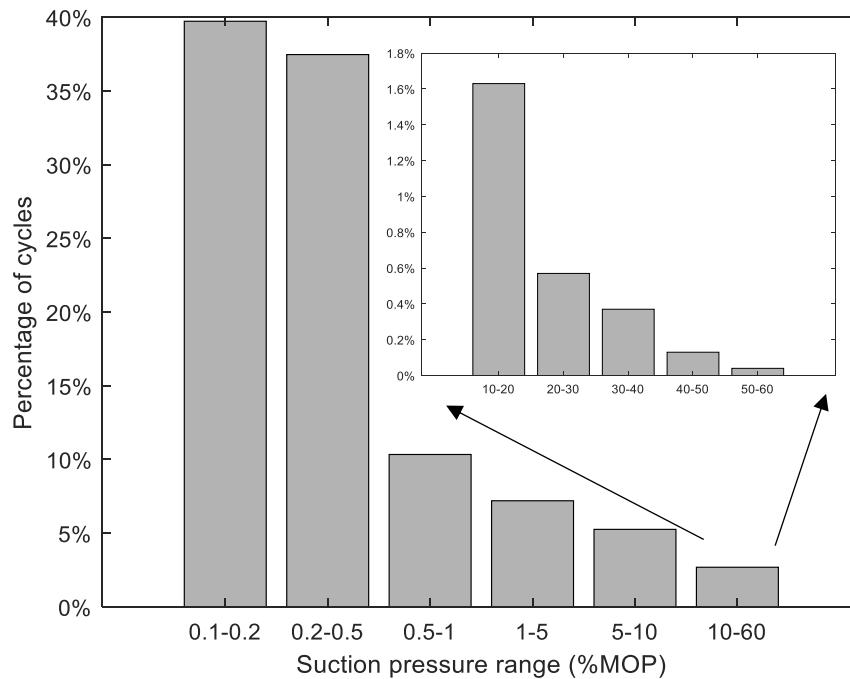
(b) Δp_s

Fig. 2.8 Histograms of Δp_d and Δp_s obtained from rainflow counting analysis
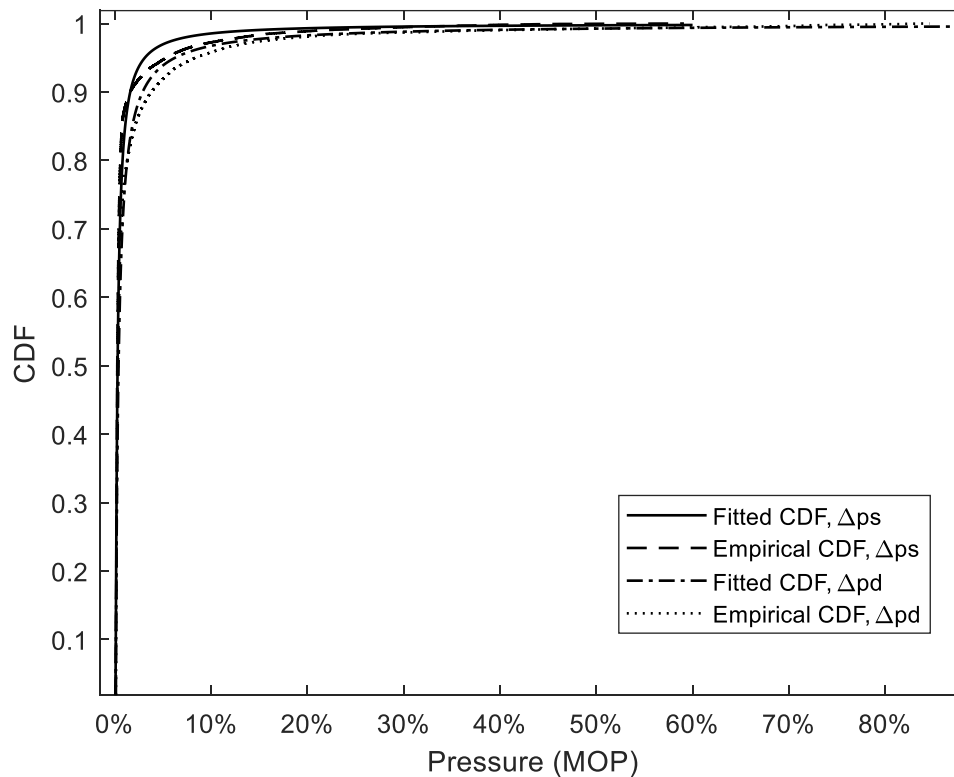
Fig 2.9 Fitted and empirical CDF of discharge and suction pressure ranges

In the context of assessing the fatigue susceptibility of seam welds in vintage electric resistance-welded (ERW) pipes, Kiefner (2002) recommended that four categories be considered for the severity of pressure cycles in pipelines with the MOP corresponding to a hoop stress level of 72%SMYS, namely very aggressive, aggressive, moderate and light. The distribution of the annual number of pressure cycles with different magnitudes of the corresponding stress ranges (calculated from the pressure ranges using the well-known Barlow equation) corresponding to each of the four severity categories is shown in Table 2.6 and also depicted in Fig. 2.10. Kiefner (2002)

suggested that if the severity of pressure cycles for a given ERW pipe falls into the aggressive or very aggressive category, then a fatigue assessment of the pipe seam weld should be considered. Although Kiefner's recommendation is applicable to ERW pipes, it is interesting to compare the discharge and suction pressure cycles for the pipeline considered in the present study with the benchmark pressure cycles as depicted in Fig. 2.10. Figure 2.10 indicates that severity of the discharge pressure cycles is generally between the very aggressive and aggressive categories, with more cycle counts in the 35 to 55%SMYS range than the aggressive benchmark but less cycle counts in the 20 to 35%SMYS range. In contrast, the suction pressure cycles is generally in the light severity category, with the cycle counts in all stress range bins except the 20 to 25%SMYS less than the corresponding benchmark counts in the light severity category.
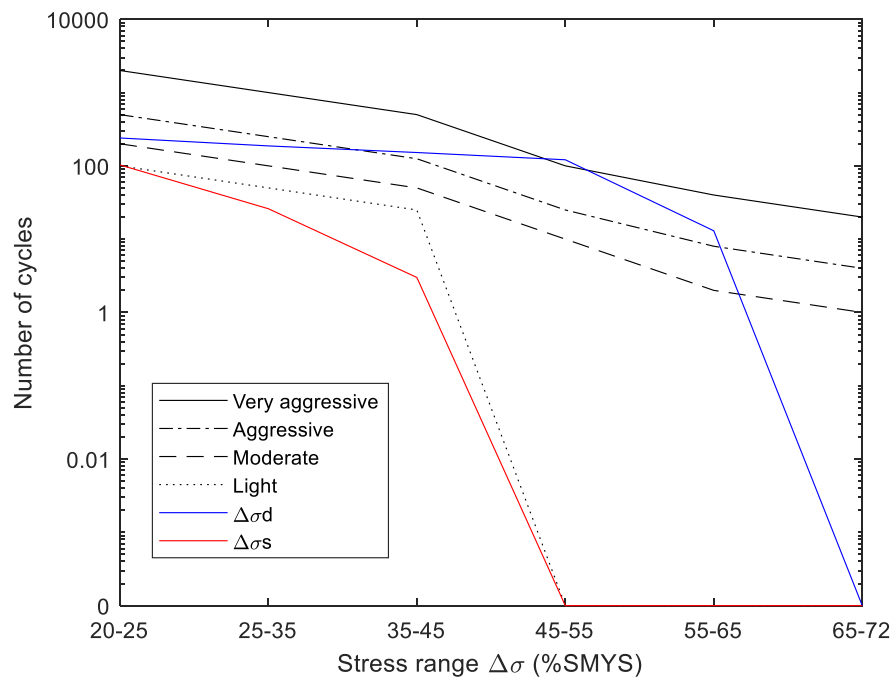
Fig 2.10 Line graph of discharge and suction stress range compared with benchmark

Table 2.6. Severity categories based on the annual pressure cycle counts proposed by Kiefner (2002)

Stress range	# of pressure cycles per year			
(%SMYS)	Very Aggressive	Aggressive	Moderate	Light
65 to 72	20	4	1	0
55 to 65	40	8	2	0
45 to 55	100	25	10	0
35 to 45	500	125	50	25
25 to 35	1000	250	100	50
20 to 25	2000	500	200	100
Total	3660	912	363	175

2.6 Conclusion

This chapter investigates the statistical characteristics of the discharge and suction pressures based on the minute-by-minute pressure records obtained from a compressor station on an in-service crude oil pipeline. The pipeline has an MOP of 9.9 MPa and a design factor of 0.8. The discharge and suction pressure records are 1.5 and 1.0 years long, respectively. The pressure records suggest that the pipeline is operating at 90% capacity, i.e. the maximum operating pressure is at 90% of MOP. For both the discharge and suction pressures, the probabilistic characteristics of the arbitrary-point-in-time pressure as well as the weekly, monthly and annual maximum pressures are derived based on the pressure records. The mean and COV of $p_{d\text{-}apt}$ are evaluated to be 57.3% and 41% MOP, respectively, and the mean and COV of $p_{s\text{-}apt}$ are 13.8%MOP and 71.9%, respectively. The Johnson SB distribution is found to be the best fit distribution for $p_{d\text{-}apt}$ and $p_{s\text{-}apt}$. The monthly and annual maximum discharge pressures can be adequately represented by a deterministic quantity equal to 90%MOP, whereas even the weekly maximum distribution of the discharge pressure could also be considered to be deterministic considering the marked drop. The weekly, monthly and annual maximum suction pressures are found to be well characterized by the beta distributions.

By considering the discharge and suction pressures as stationary stochastic processes, the autocorrelation and PSD functions of the discharge and suction pressures are evaluated based on the pressure records. The autocorrelation function of the discharge pressure is well characterized by the exponential correlation function with a correlation length equal to 439 minutes, whereas the γ-exponential function adequately characterizes the autocorrelation function of the suction pressure with a correlation length of 966 minutes. The analytical expression of the PSD function corresponding to the exponential autocorrelation function for the discharge pressure is obtained and agrees very well with the numerically evaluated PSD function using Welch's method. The PSD function for the suction pressure is also numerically evaluated using Welch's method. The bandwidth parameter α_2 is also calculated for both discharge and suction pressures and indicates that both are wide-band processes. The rainflow counting method is applied to obtain the pressure range distributions associated with the discharge and suction pressures. The Frechet distributions are found to fit well the pressure ranges of the discharge and suction pressures. The discharge and suction pressure ranges are further compared with the benchmark pressure cycle counts proposed in the literature to identify their severity. The results suggest that the discharge pressure ranges fall in between the very aggressive and aggressive categories, whereas the suction pressure ranges can be characterized as light severity.

The findings of the present study provide valuable information of the basic uncertainties involved in the reliability-based integrity management of oil and gas pipelines with respect to various threats such as corrosion, third-party interference and fatigue.

References

Ahammed M, Melchers RE. Reliability estimation of pressurised pipelines subject to localised corrosion defects. International Journal of Pressure Vessels and Piping. 1996 Dec 1;69(3):267-72.

Alexander CR, Kiefner JF. Effects of smooth and rock dents on liquid petroleum pipelines. In1999 API Pipeline Conference, Dallas, Texas 1997 Oct 10.

ASTM E1049-85(2017), Standard Practices for Cycle Counting in Fatigue Analysis, ASTM International, West Conshohocken, PA, 2017

Bendat JS, Piersol AG. Random Data, Wiley Series in Probability and Statistics.

Canadian Standard Association (CSA) Z662-15, Oil and gas pipeline system, Canadian Standard Association, Mississauga, ON, Canada. 2016

EasyFit Version 5.6 (Software) [e]MathWave Technologies

Jiao G, Sotberg T, Igland R. SUPERB 2M statistical data-basic uncertainty measures for reliability analysis of offshore pipelines. SUPERB project report. 1995:35-8.

Johnson NL. Systems of frequency curves generated by methods of translation. Biometrika. 1949 Jun 1;36(1/2):149-76.

Kariyawasam S, Huyse L. Providing Safety: Using Probabilistic or Deterministic Methods. InInternational Pipeline Conference 2012 Sep 24 (Vol. 45158, pp. 725-734). American Society of Mechanical Engineers.

Keshtegar B, Seghier ME, Zhu SP, Abbassi R, Trung NT. Reliability analysis of corroded pipelines: novel adaptive conjugate first order reliability method. Journal of Loss Prevention in the Process Industries. 2019 Nov 1;62:103986.

Kiefner JF. Dealing with low-frequency-welded ERW pipe and flash-welded pipe with respect to HCA-related integrity assessments. In ASME 2002 Engineering Technology Conference on Energy 2002 Feb 4 (pp. 699-706). American Society of Mechanical Engineers Digital Collection.

Kiefner JF, Kiefner BA, Vieth PH. Analysis of DOT reportable incidents for hazardous liquid Pipelines, 1986 through 1996. American Petroleum Institute Publication. 1999 Jan 7;1158.

Kiefner JF, Mesloh RE, Kiefner BA. Analysis of DOT reportable incidents for gas transmission and gathering system pipelines, 1985 through 1997. Pipeline Research Council International, Catalogue. 2001 Mar 20(L51830E).

Nessim M. and Zhou W. Guidelines for reliability-based design and assessment of onshore natural gas pipelines. 2005 GRI-04/0229

Nessim M, Zhou W, Zhou J, Rothwell B, McLamb M. Target reliability levels for design and assessment of onshore natural gas pipelines. InInternational Pipeline Conference 2004 Jan 1 (Vol. 41766, pp. 2501-2512).

Rasmussen CE, Williams CK. I (2006) Gaussian Processes for Machine Learning.

Rosenfeld MJ, Pepper JW, Leewis K. Basis of the new criteria in ASME B31. 8 for prioritization and repair of mechanical damage. InInternational Pipeline Conference 2002 Jan 1 (Vol. 36207, pp. 647-658).

Rosenfeld MJ, Zand B, Steiner A. Power Spectral Density Analysis of Pipeline Pressures for Probabilistic Assessment. InInternational Pipeline Conference 2020 Sep 28 (Vol. 84447, p. V001T03A076). American Society of Mechanical Engineers.

Solomon Jr OM. PSD computations using Welch's method. NASA STI/Recon Technical Report N. 1991 Dec;92:23584.

Teixeira AP, Soares CG, Netto TA, Estefen SF. Reliability of pipelines with corrosion defects. International Journal of Pressure Vessels and Piping. 2008 Apr 1;85(4):228-37.

Vanmarcke E. Random fields: analysis and synthesis. World Scientific Publishing Co Pte. Ltd., Singapore 596224, 2010.

Zhang H, Tian ZW. Reliability assessment of corroded pipeline considering multiple defects interaction based on an artificial neural network method. In 2020 Asia-Pacific International Symposium on Advanced Reliability and Maintenance Modeling (APARM) 2020 Aug 20 (pp. 1-6). IEEE.

Zhang S, Zhou W. System reliability of corroding pipelines considering stochastic process-based models for defect growth and internal pressure. International Journal of Pressure Vessels and Piping. 2013 Nov 1;111:120-30.

Zhang S, Zhou W. Probabilistic characterisation of metal-loss corrosion growth on underground pipelines based on geometric Brownian motion process. Structure and Infrastructure Engineering. 2015 Feb 1;11(2):238-52.

Zhou W. System reliability of corroding pipelines. International Journal of Pressure Vessels and Piping. 2010 Oct 1;87(10):587-95.

3 Reliability analyses of corroding pipelines using different approaches to characterize uncertainties in internal pressure

3.1 Introduction

Reliability-based corrosion management programs are more and more adopted by pipeline operators in recent years because of its effectiveness to address various uncertainties involved in the decision-making process such as uncertainties associated with the pipe material properties, corrosion growth rates and internal operating pressure (Zhang et al. 2014, Adianto et al. 2018, Al-Amin et al. 2020). The corrosion management program of a given pipeline typically consists of three steps. In the first step, high-resolution inline inspections (ILI) of the pipeline are carried out periodically to detect and size corrosion anomalies on the pipeline. Based on the ILI data, pipeline integrity engineers develop probabilistic corrosion growth models (Zhang et al. 2012) and conduct reliability analyses to evaluate the failure probability of the pipeline as a function of time. In the final step, the failure probability of the pipeline is compared with the allowable failure probability to determine if corrosion mitigation actions are required and how such mitigation actions can be scheduled given various constraints in terms of the maintenance budget and manpower (Gong and Zhou 2018).

The internal pressure is the main operational load for pipelines. Probabilistic characteristics of the internal pressure are one of the key uncertainties in the reliability analysis of corroding pipelines (Zhou 2010; Zhang and Zhou 2014). For natural gas pipelines operating at capacity, the Canadian pipeline standard CSA Z662-19 (CSA 2019) suggests that the ratio between the annual maximum internal pressure (p_{ae}) and Maximum Operating Pressure (MOP), p_{ae}/MOP, be represented by a beta distribution with a mean of 0.993 and a coefficient of variation (COV) of 3.4%, lower and upper bounds of 80 and 110%, respectively. Jiao et al. (1995) recommended that p_{ae}/MOP for gas

pipelines be characterized by a Gumbel distribution with a mean between 1.03 and 1.07 and a COV between 1 and 2%. Because of the difference in the compressibility of gas and liquid, the statistics of internal pressure of liquid pipelines (e.g. crude oil pipelines) are different from those of gas pipelines; however, such statistics are unavailable in CSA Z662-19. There are a wide range of assumptions in the literature concerning probabilistic characteristics of the pipeline internal pressure. For example, Keshtegar et al. (2019) assumed the internal pressure to follow a normal distribution with a COV of 10%; Teixeira et al (2008) assumed the internal pressure to follow a Gumbel distribution with a mean of 0.97MOP and a COV of 7%, and Ahammed and Melchers (1996) assumed the pressure to follow a normal distribution with a COV of 5%. It is unclear if the above statistics are recommended based on pressure data collected from actual pipelines; it is also unclear if these statistics apply to the internal pressure of gas or liquid pipelines. Although the pipeline internal pressure is characterized as a time-independent random variable in a majority of studies reported in the literature, the internal pressure inevitably fluctuates with time and should be treated rigorously as a stochastic process in the reliability analysis. Zhou (2010) assumed the internal pressure to be approximated by a discrete Ferry-Borges process with a sequence of independent and identically distributed (IID) random variables each representing the annual maximum internal pressure. Zhang and Zhou (2013) employed the Poisson square wave process to characterize the internal pressure in carrying out the reliability analysis of corroding pipelines.

The present study obtained from a Canadian pipeline company the minute-by-minute pressure records at the discharge and suction ends of a pump station on a crude oil transmission pipeline in the company's pipeline network. The pipeline has an MOP of 9.964 MPa and a design factor of 0.8; the meaning of the latter has been explained in Chapter 2. Statistical analyses of the pressure records have been carried out to derive the probabilistic characteristics of the arbitrary-point-in-

time pressures as well as the weekly, monthly and annual maximum discharge and suction pressures. Furthermore, the discharge and suction pressures are considered as stationary stochastic processes. The marginal probability distributions as well as correlation functions of the discharge and suction pressures are derived based on the pressure records. Detailed analysis results are reported in Chapter 2.

The objective of the study reported in Chapter 3 is to investigate the implications of probabilistic characteristics of the internal pressure reported in Chapter 2 for the reliability analysis of corroding pipelines. To this end, two hypothetical crude oil pipeline examples are considered in the analysis. Both examples are assumed to have the same MOP as the real pipeline from which the pressure records are obtained. Due to confidentiality reasons, the attributes of the real pipeline are not disclosed; therefore, the attributes of the two hypothetical pipeline examples are assumed according to the MOP. It is assumed that the example pipelines have been subjected to recent ILIs that report sizes of corrosion defects on the pipelines. The probabilities of failure of representative corrosion defects are then evaluated based on ILI-reported defect sizes and corrosion growth rates that are commonly assumed in the literature (Zhou 2010; Gong and Zhou 2017). The failure of a pipeline at a corrosion defect is defined as the pressure containment capacity, i.e. burst capacity, of the pipeline at the corrosion defect is below the internal pressure of the pipeline. The PCORRC model (Huang and Zhou 2012), which is a well-known semi-empirical burst capacity model for corroded pipelines, is adopted to evaluate the burst capacity of the pipeline at the defect. The pipeline internal pressure is considered as a random variable or stochastic process in the reliability analysis. The probabilistic characteristics of the internal pressure reported in Chapter 2 as well as in the literature are considered in the reliability analysis, and the corresponding failure probabilities are compared to shed light on the impact of the internal pressure on the evaluated failure

probability. The first-order and second-order reliability method (FORM and SORM) (Der Kiureghian 2005; Zhou et al. 2018) and simple Monte Carlo simulation (MCS) (Melchers 1999) are employed to evaluate the failure probabilities of the corroding pipelines as a function of time.

The rest of Chapter 3 is organized as follows. Section 3.1 describes the reliability analysis methodology including the limit state function, PCORRC model and details of using the FORM, SORM and MCS to evaluate the failure probability of corroding pipelines; Section 3.2 describes the example pipelines and analysis results, followed by concluding remarks in Section 3.4.

3.2 Methodology

3.2.1 Limit state function

The limit state function, g, for a corrosion defect on a pipeline is expressed as follows:

$$g = r - p \tag{3.1}$$

where r is the burst capacity at the defect; p is the internal pressure, and $g \leq 0$ represents failure, i.e. burst. It is emphasized that both r and p depend on time t; however, for notational simplicity, the dependence is made implicit in Eq. (3.1). The PCORRC model is used to compute r:

$$r = \xi \frac{2wt\sigma_u}{D} \left[1 - \frac{d_{max}}{wt} \left(1 - \exp\left(\frac{-0.157l}{\sqrt{\frac{D(wt - d_{max})}{2}}} \right) \right) \right] \tag{3.2}$$

where D and wt denote the pipe outside diameter and wall thickness, respectively; σ_u denotes the tensile strength of the pipe steel; d_{max} and l denote the defect depth and length, respectively (Fig. 1); and ξ is the model error associated with the PCORROC model (Bao and Zhou 2020). The dependence of r on t derives from the fact that both d_{max} and l in general grow with time. Consider the time of ILI as time zero. For simplicity and consistency with typical corrosion assessment practice in the industry, the linear growth model, i.e. with a constant growth rate, is adopted for

the defect depth in the present study. Furthermore, the defect length is assumed to remain the same over time, i.e. no length growth. It follows that $d_{max}(t)$ at year t since the time of ILI can be expressed as:

$$d_{max}(t) = d_{max0} + g_d t \tag{3.3}$$

where d_{max0} is the defect depth at the time of ILI, and g_d denotes the depth growth rate per year.
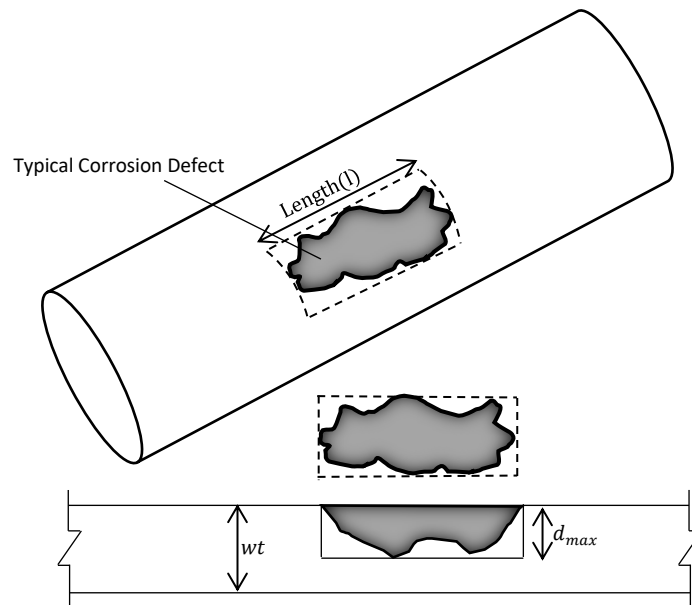
Fig 3.1. Typical corrosion defect

3.2.2 Reliability analysis

The instantaneous failure probability of the corrosion defect at year t is denoted as $P_{f,i}(t) = $ Prob $[g(t) \leq 0]$. The well-known FORM can be employed to evaluate $P_{f,i}(t) \approx \Phi(-\beta(t))$, where $\Phi(\bullet)$ is the standard normal distribution function, and $\beta(t)$ is the so-called reliability index obtained from the FORM and represents the shortest distance from the limit state surface (i.e. $g(t) = 0$) to the origin in the standard normal space (Zhou et al. 2017). Because the FORM approximates the limit state surface with a hyperplane, the accuracy of the FORM may not be sufficient for limit state

surfaces with large curvatures. In this case, the SORM can be used to improve the accuracy of the FORM.

If the internal pressure is assumed to be a (time-independent) random variable, then the failure probability of the corrosion defect up to year t since time zero, $P_f(t)$, equals the instantaneous failure probability at year t, i.e. $P_f(t) = P_{f,i}(t)$ (Zhang and Zhou 2014). This is because the burst capacity r monotonically decreases with time as corrosion defects cannot rehabilitate themselves. It follows that $P_f(t)$ can be easily computed using the FORM/SORM by assuming the internal pressure to be time independent. If the internal pressure is treated rigorously as a stochastic process, then $P_f(t)$ is defined as $P_f(t) = \text{Prob}[g(\tau) \leq 0, \ni \tau \in [0, t]]$, where the symbol "$\ni$" means "there exists". The system reliability approach can be employed to approximately evaluate $P_f(t)$ by first selecting n points within the interval $[0, t]$ with $0 \leq \tau_1 < \tau_2 < \ldots < \tau_n \leq t$. Then,

$$P_f(t) = \text{Prob}[g(\tau_1) \leq 0 \cup g(\tau_2) \leq 0 \ldots \cup g(\tau_n) \leq 0] \tag{3.4}$$

That is, $P_f(t)$ is the failure probability of a series system consisting of n components, each of which is associated with the limit state function $g(\tau_i)$ ($i = 1, 2, \ldots, n$). Note that the n limit state functions are correlated because they share the same random variables (e.g. the pipe wall thickness and tensile strength) and because the defect sizes and internal pressures at different times are statistically dependent. A recently-developed efficient system reliability analysis methodology based on the FORM (Zhou et al. 2017; Gong and Zhou 2018; Gong and Frangopol 2019) can be employed to evaluate $P_f(t)$ based on Eq. (3.4). The essence of this approach is to use the FORM to evaluate the failure probability of each component by involving random variables associated with the particular component only. The solution obtained from the FORM for an individual component is then mapped to the space of the random variables associated with all the components to facilitate the evaluation of the correlation between different components. Finally, individual

components are combined successively into equivalent components to facilitate the evaluation of the system reliability.

Alternatively, MCS can be employed to evaluate $P_f(t)$ by considering the internal pressure as a stochastic process. In this case, realizations of the internal pressure and the time-independent random variables involved in the limit state function need to be generated using suitable techniques. In the present study, an improvement spectral representation method proposed by Masters and Gurly (2003) is adopted to generate realizations of the internal pressure by assuming the internal pressure as a stationary stochastic process with known marginal distribution function and power spectral density (PSD) function. Masters and Gurly's method, referred to as the iterative spectral correction method (ISCM) hereafter, generates realizations of a non-Gaussian stationary process by matching the prescribed PSD function while iteratively correcting the probability distribution of the generated samples until it converges to the prescribed marginal distribution within a pre-defined tolerance.

3.3 Example pipelines and probabilistic characteristics of basic parameters

The attributes of the two example pipelines considered in the reliability analysis are summarized in Table 1. As explained in the Introduction, both examples are assumed to have the same MOP of 9.964 MPa and be subjected to the time-varying discharge pressure as analyzed in Chapter 2. Examples #1 and #2 are assumed to have design factors (*FS*) of 0.72 and 0.8, respectively. The nominal diameters (D_n) of examples #1 and #2 are assumed to be 508 and 914 mm (20 and 36 inches), respectively, representing medium- and large-diameter pipelines. The pipe steel grades of examples #1 and #2 are assumed to be X52 and X70, respectively, corresponding to the specified minimum yield strength (SMYS) of 359 and 483 MPa, respectively. The specified minimum tensile strength (SMTS) of the X52 and X70 steels are 455 and 565 MPa, respectively. Given D_n,

SMYS, MOP and the design factor, the nominal pipe wall thickness (wt_n) is determined using the well-known Barlow equation as follows:

$$wt_n = \frac{D_n \cdot MOP}{2 \cdot FS \cdot SMYS} \tag{3.5}$$

Table 3.1. Attributes of the two example pipelines

Example	Steel Grade	SMYS (MPa)	wt_n (mm)	D_n (mm)	Design Factor	MOP (MPa)
#1	X52	359	9.80	508	0.72	9.964
#2	X70	481	11.78	914	0.80	9.964

The probabilistic characteristics of the discharge pressure have been analyzed in Chapter 2. Let $p_{d\text{-}apt}$, $p_{d\text{-}we}$, $p_{d\text{-}me}$ and $p_{d\text{-}ae}$ denote the arbitrary-point-in-time, weekly maximum, monthly maximum and annual maximum discharge pressures, respectively. As reported in Chapter 2, the analysis of the minute-by-minute discharge pressure record suggests that $p_{d\text{-}apt}$ can be characterized by a Johnson SB (JSB) distribution with the corresponding cumulative distribution function (CDF), $F(p_{d\text{-}apt})$, given by

$$F\left(p_{d-apt}\right) = \Phi\left(\gamma + \delta\, ln\left(\frac{z}{1-z}\right)\right) \tag{3.6}$$

where $z = \frac{p_{d-apt} - \xi}{\lambda}$; $\Phi(\bullet)$ denotes the CDF of the standard normal distribution, and ξ, λ, δ and γ are the distribution parameters, equal to 0, 0.9MOP, 0.69 and -0.53, respectively, as reported in Chapter 2. Note that the JSB distribution is bounded with the lower bound equal to ξ and the upper bound equal to $\xi + \lambda$. The analysis of the discharge pressure record further indicates that $p_{d\text{-}we}$, $p_{d\text{-}me}$ and $p_{d\text{-}ae}$ all have negligibly small variability such that they can be approximated by a deterministic quantity of 0.9MOP.

If the discharge pressure is considered to be a stationary stochastic process, then its marginal distribution follows $F(p_{d\text{-}apt})$ as given by Eq. (3.5). The single-sided PSD function of the discharge pressure, $S_d(f)$ ($f \geq 0$), is given by,

$$S_d(f) = \frac{4(\sigma_{d-apt})^2 \tau_{0d}}{(2\pi f \tau_{0d})^2 + 1} \tag{3.7}$$

where $\sigma_{d\text{-}apt}$ is the standard deviation of $p_{d\text{-}apt}$ and estimated to be 0.23MOP based on samples from the discharge pressure record, and τ_{0d} is the correlation length of the discharge pressure, which is estimated to 439 minutes as reported in Chapter 2.

The reliability analysis is carried out by considering a single corrosion defect on each of the two example pipelines. The ILI-reported depth and length (d_{max0} and l) of the defect are assumed to equal $0.3wt_n$ and 100 mm, respectively. The analysis is then carried out to estimate the failure probabilities of the defect for a period of five years after the time of ILI. The probabilistic characteristics of the basic parameters involved in the reliability analysis except the internal pressure are summarized in Table 2. Note that uncertainties associated with d_{max0} and l reflect the measurement error associated with the ILI tool. Several scenarios in terms of the uncertainty of the internal pressure (p) are considered in the reliability analysis, as summarized in Table 3. Note that scenario #1 is considered the most accurate representation of the uncertainty in the internal pressure; therefore, the corresponding failure probabilities are the benchmark results. Scenario #2 considers the internal pressure as a deterministic quantity based on findings reported in Chapter 2; therefore, the reliability analysis is greatly simplified whereby the failure probability up to time t equals the instantaneous failure probability at time t. The FORM can be easily carried out to estimate the instantaneous failure probability. The MCS is also conducted for scenario #2 to verify the accuracy of the FORM results. Scenarios #3-#5 are sensitivity cases to investigate the impact

of the uncertainty in p on the failure probability. Scenarios #3 and #4 consider p to be random variables with different probability distributions as suggested in the literature, whereas scenario #5 characterizes p as a Ferry-Borges process (Zhou 2010) consisting of independent, identically distributed (iid) pulses represented by the annual maximum pressure that follows a Gumbel distribution with a mean of 1.03MOP and a COV of 1%. Each MCS involves a total of 10^5 simulation trials. In scenario #1, the time step used to generate samples of p in MCS is 3 hrs.

Table 3.2. Probabilistic characteristics of basic parameters involved in the reliability analysis

Parameter	Distribution	Mean	COV (%)	Sources
wt	Normal	t_n	1.50	Gong (2017)
D	Deterministic	D_n	-	CSA (2019)
σ_u	Normal	1.1SMTS	3.50	Gong 2017
l	Normal	100 (mm)	15	Gong 2017
d_{max0}	Normal	30%wt	20	Assumed
ξ	Gumbel	1.079	26.4	Zhou 2012
g_d	Lognormal	0.3 (mm/year)	50	Zhou 2010
p	Johnson SB process	0.589MOP	41.15	Chapter 2

Table 3.3 Scenarios of uncertainty in p considered in the reliability analysis

Scenario	Consideration of uncertainty in p	Source	Reliability analysis methodology
#1	Stochastic process with the CDF given by Eq. (3.6) and PSD function given by Eq. (3.7)	Present study	MCS
#2	Deterministic value equal to 0.9MOP	Present study	FORM and MCS
#3	Gumbel-distributed random variable with a mean of 1.0MOP and a COV of 10%	Teixeira et al. (2008)	MCS
#4	Normally distributed random variable with a mean of 1.0MOP and a COV of 10%	Keshtegar et al. (2019)	MCS
#5	Ferry-Borges process with iid annual pulses represented by a Gumbel random variable with a mean of 1.03MOP and a COV of 1%	Zhou (2010)	MCS

The computed failure probabilities of the two example pipelines considering different scenarios of the uncertainty in the internal pressure are depicted in Fig. 3.2. The figure indicates that the failure probabilities corresponding to scenario #2 are somewhat higher than the benchmark values, i.e. corresponding to scenario #1, which suggests that it is acceptable to evaluate the failure probability of corroding pipelines by considering the probabilistic characteristics of the annual extreme internal pressure as opposed to treating rigorously the internal pressure as a stochastic process with the corresponding CDF and PSD function. The advantage of scenario #2 is its high computational efficiency compared with scenario #1. The comparison of the FORM and MCS results corresponding to scenario #2 indicate that the two methods result in almost identical failure probabilities for example #1 and that the FORM results are marginally lower than the MCS results for example #2. This confirms the accuracy and suitability of the FORM for the reliability analysis of corroding pipelines. On the other hand, the failure probabilities corresponding to scenarios #3-#5 are about one order of magnitude higher than the benchmark values. This underscores the importance of appropriately characterizing the uncertainty in the internal pressure in the reliability analysis of corroding pipelines. A comparison of the results corresponding to scenarios #3 and #4 suggests that the failure probability is not sensitive to the distribution of the internal pressure if its mean and COV remain the same.
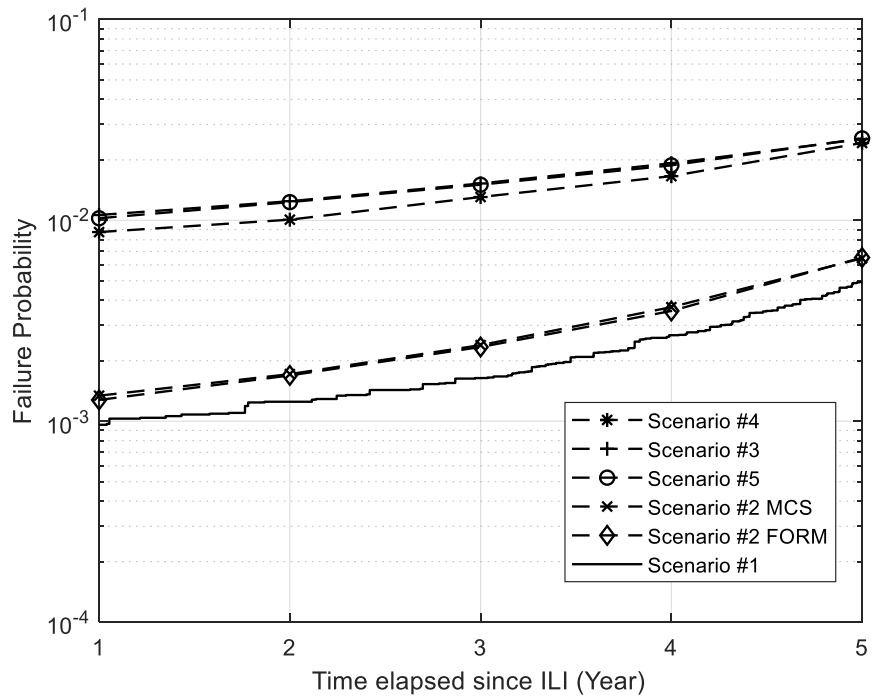
(a) Example 1
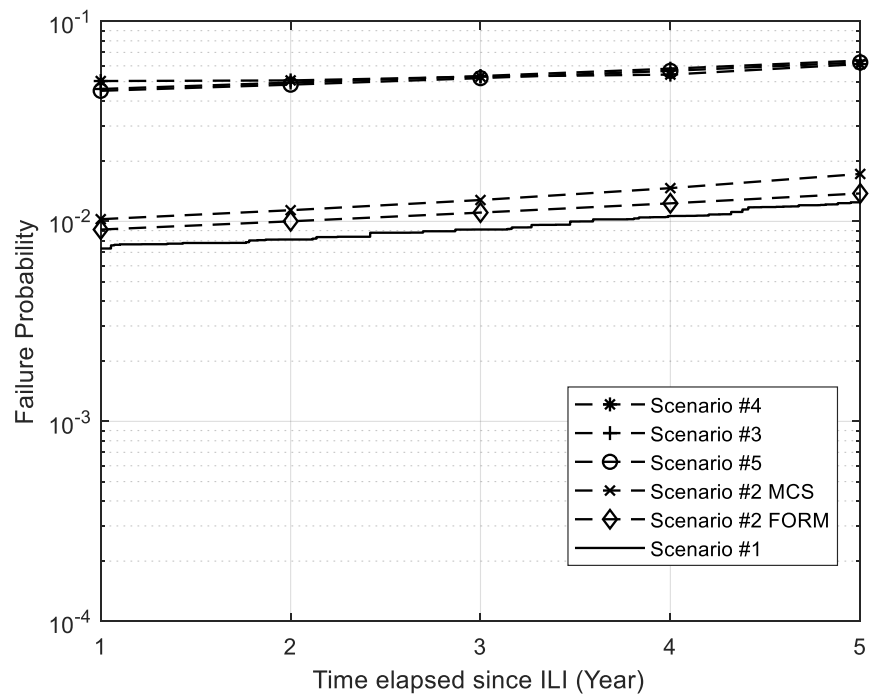
(b) Example 2

Fig. 3.2 Failure probabilities of two example pipelines considering different scenarios in terms of the uncertainty in the internal pressure

3.4 Comparison between FORM and simulation results

Because it is relatively time-consuming to evaluate the failure probabilities corresponding to scenario #1 using MCS, the FORM-based system reliability method as proposed in the recent literature (Zhou et al. 2017; Gong and Zhou 2018; Gong and Frangopol 2019), referred to as the improved equivalent component method, is employed to evaluate the failure probabilities. To this end, the number of components included in the system reliability analysis (see Eq. 3.(4)) within the analysis period of five years is assumed to be 30 (i.e. an equal interval of 2 months between consecutive components), 40 (i.e. an equal interval of 1.5 months between consecutive components), 60 (i.e. an equal interval of one month between consecutive components), 130 (i.e. an equal interval of two weeks between consecutive components) or 260 (i.e. an equal interval of one week between consecutive components). The corresponding failure probabilities are depicted in Fig. 4 for the two example pipelines. For comparison, the benchmark failure probabilities obtained from MCS are also shown in the figure. Figure 4 indicates that the improved equivalent component method results in unreliable predictions of the failure probabilities compared with the benchmark values. This may be explained as follows. Gong (2017) indicated that the improved equivalent component method leads to relatively large errors if the limit states corresponding to different components are highly correlated with the correlation coefficient greater than 0.9. Because corrosion is a slow growth process, there is a small difference between the corrosion depths for different components, which implies high correlations between different components.

It is observed from Fig. 4 that the accuracy of failure probabilities evaluated using the improved equivalent component method depends to a large degree on the number of components. The failure

probability evaluated increases with the number of components included in the analysis. For example # 2 (i.e. the large diameter pipeline), the failure probability is relatively larger, it is seen that only the 30-component case underestimates the result compared with the benchmark by 1.2%; the 40-component case overestimates the benchmark result by 6.1%; the 60-component case overestimates the benchmark by 23.4%; the 130-component case overestimates the benchmark by 62.4%, and the 260-component case overestimates by 103.9%. On the other hand, for example #1 (i.e. the medium diameter pipeline), where the failure probability is relatively small, the 260-component and 130-compoent cases result in the most accurate predictions, whereas errors associated with the other cases range from 20 to 60%.
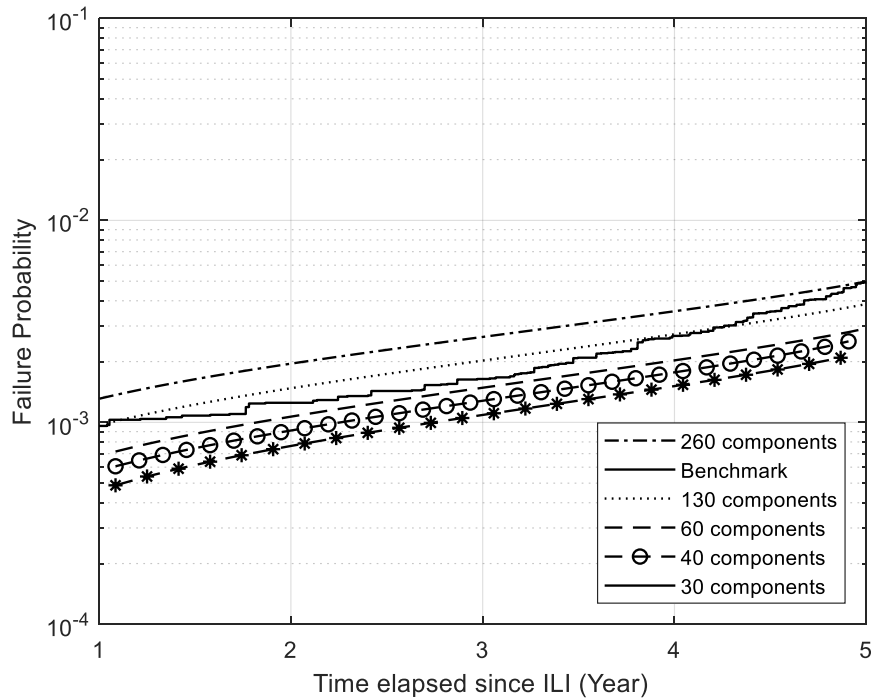
(a) Example #1
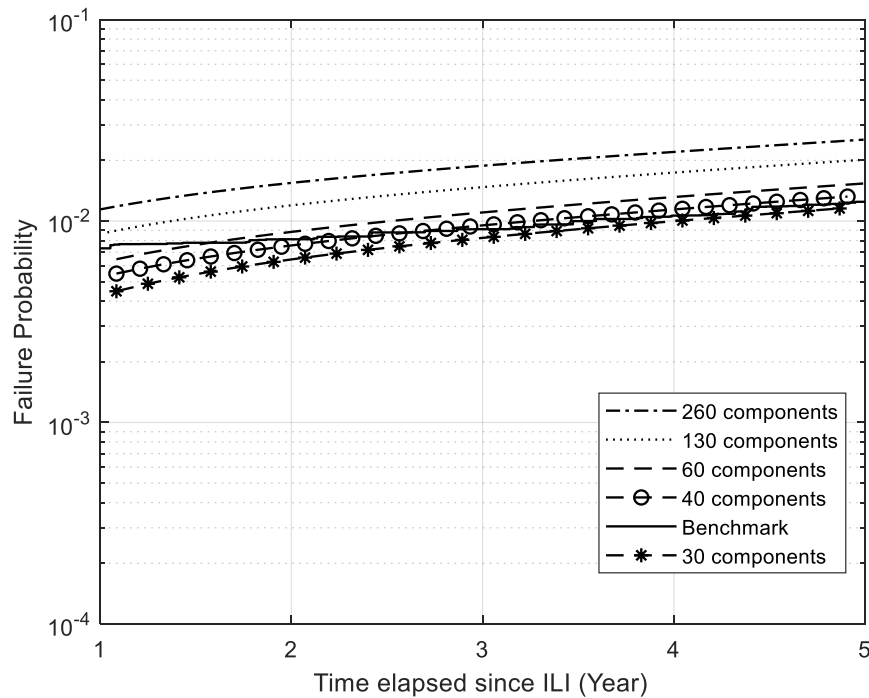
(b) Example #2

Fig. 3.3 Failure probabilities evaluated using the FORM-based system reliability method compared with the benchmark values obtained from MCS

3.5 Conclusion

This chapter investigates the reliability of corroded oil pipeline considering arbitrary-point-in-time pressure as stochastic process with multiple reliability methods and compares it with different pressure assumptions. Two examples of oil pipeline representing smaller and larger size are selected with the same MOP and different parameters (wall thickness, diameter, steel grade, etc.). Discharge pressure distribution (Johnson SB) and correlation structure are chosen from chapter 2 of the thesis. Then, ISCM is used to generated discretized pressure in every three hours for five years period where good accuracy is achieved after 5 iterations. Simulation based reliability is compared between pressure as a stochastic process (the benchmark) and extreme value pressure

are given where the difference at the end of fifth year is 29.41% and 29.13% for two cases representing smaller and larger pipe size. Three previously used pressure distribution from several papers are also compared by simulation where all of them gives considerably higher failure results than pressure as stochastic process. A major reason is those previously used pressure is considered pipeline operating under MOP while our record is under 0.9 MOP. However, as the upper bound of pressure varies as the operation conditions change, more operations should be implemented as opposed to one to better incorporate the actual environment.

FORM is also tried as an alternative evaluation of the failure probability. on the improved equivalent component method is also applied with the corresponding results compared with MCS results. The results indicate that the accuracy of the improved equivalent component method depends largely on the number of components considered in the analysis. The error can be significant if the number of components is not selected properly. This may be due to the fact that different components are highly correlated due to the slow growth nature of the corrosion process. However, for extreme value pressure distribution, FORM gives a fairly accurate result comparing with the benchmark with small difference of 27.45% and 5.22% for smaller and larger pipe size.

The findings of this study provide a method to consider internal pressure as a stochastic process in reliability analysis of corroded pipeline. The results show evidence of potential conservativeness of corrosion failure considering pressure as maximum probable value which is independent of time.

References

Adianto R, Nessim M, Kariyawasam S, Huang T. Implementation of Reliability-Based Criteria for Corrosion Assessment. In2018 12th International Pipeline Conference 2018 Sep 24. American Society of Mechanical Engineers Digital Collection.

Ahammed M, Melchers RE. Reliability estimation of pressurised pipelines subject to localised corrosion defects. International Journal of Pressure Vessels and Piping. 1996 Dec 1;69(3):267-72.

Al-Amin M, Zhang S, Kariyawasam S, Yan JZ, Matchim T. Achieving Consistent Safety by Using Appropriate Safety Factors in Corrosion Management Program. In2020 13th International Pipeline Conference 2020 Sep 28. American Society of Mechanical Engineers Digital Collection.

Brzakała W, Puła W. A probabilistic analysis of foundation settlements. Computers and Geotechnics. 1996 Jan 1;18(4):291-309.

Canadian Standard Association (CSA) Z662-15, Oil and gas pipeline system, Canadian Standard Association, Mississauga, ON, Canada. 2016

Chan CL, Low BK. Practical second-order reliability analysis applied to foundation engineering. International Journal for Numerical and Analytical Methods in Geomechanics. 2012 Aug 10;36(11):1387-409.

Cho SE. Probabilistic stability analyses of slopes using the ANN-based response surface. Computers and Geotechnics. 2009 Jun 1;36(5):787-97.

Der Kiureghian A. First-and second-order reliability methods. Engineering design reliability handbook. 2005;14.

Du X, Hu Z. First order reliability method with truncated random variables. Journal of Mechanical Design. 2012 Sep 1;134(9).

Fiessler B, Neumann HJ, Rackwitz R. Quadratic limit states in structural reliability. Journal of the Engineering Mechanics Division. 1979 Aug;105(4):661-76.

Gollwitzer S, Rackwitz R. Equivalent components in first-order system reliability. Reliability Engineering. 1983 Jan 1;5(2):99-115.

Gong C, Frangopol DM. An efficient time-dependent reliability method. Structural Safety. 2019 Nov 1;81:101864.

Gong C, Zhou W. Improvement of equivalent component approach for reliability analyses of series systems. Structural Safety. 2017 Sep 1;68:65-72.

Gong C, Zhou W. Multi-objective maintenance strategy for in-service corroding pipelines using genetic algorithms. Structure and Infrastructure Engineering. 2018 Nov 2;14(11):1561-71.

Grigoriu M. Simulation of stationary non-Gaussian translation processes. Journal of engineering mechanics. 1998 Feb;124(2):121-6.

Jiao G, Sotberg T, Igland R. SUPERB 2M statistical data-basic uncertainty measures for reliability analysis of offshore pipelines. SUPERB project report. 1995:35-8.

Kang WH, Song J. Evaluation of multivariate normal integrals for general systems by sequential compounding. Structural Safety. 2010 Jan 1;32(1):35-41.

Keshtegar B, Seghier ME, Zhu SP, Abbassi R, Trung NT. Reliability analysis of corroded pipelines: novel adaptive conjugate first order reliability method. Journal of Loss Prevention in the Process Industries. 2019 Nov 1;62:103986.

Low BK, Tang WH. Efficient spreadsheet algorithm for first-order reliability method. Journal of engineering mechanics. 2007 Dec;133(12):1378-87.

Masters F, Gurley KR. Non-Gaussian simulation: cumulative distribution function map-based spectral correction. Journal of engineering mechanics. 2003 Dec;129(12):1418-28.

Phoon KK, Huang HW, Quek ST. Simulation of strongly non-Gaussian processes using Karhunen–Loeve expansion. Probabilistic engineering mechanics. 2005 Apr 1;20(2):188-98.

Roscoe K, Diermanse F, Vrouwenvelder T. System reliability with correlated components: Accuracy of the Equivalent Planes method. Structural Safety. 2015 Nov 1;57:53-64.

Sahraoui Y, Khelif R, Chateauneuf A. Maintenance planning under imperfect inspections of corroded pipelines. International journal of pressure vessels and piping. 2013 Apr 1;104:76-82.

Teixeira AP, Soares CG, Netto TA, Estefen SF. Reliability of pipelines with corrosion defects. International Journal of Pressure Vessels and Piping. 2008 Apr 1;85(4):228-37.

Xiu D, Karniadakis GE. The Wiener--Askey polynomial chaos for stochastic differential equations. SIAM journal on scientific computing. 2002;24(2):619-44.

Yamazaki F, Shinozuka M. Digital generation of non-Gaussian stochastic fields. Journal of Engineering Mechanics. 1988 Jul;114(7):1183-97.

Zhang S, Zhou W. System reliability of corroding pipelines considering stochastic process-based models for defect growth and internal pressure. International Journal of Pressure Vessels and Piping. 2013 Nov 1;111:120-30.

Zhang S, Zhou W. An efficient methodology for the reliability analysis of corroding pipelines. Journal of Pressure Vessel Technology. 2014 Aug 1;136(4).

Zhang S, Zhou W, Al-Amin M, Kariyawasam S, Wang H. Time-dependent corrosion growth modeling using multiple in-line inspection data. Journal of Pressure Vessel Technology. 2014 Aug 1;136(4).

Zhao, H. et al (2019) "Nonparametric and parametric methods of spectral analysis" MATEC Web of Conferences 283, 07002 (2019)

Zhou W. System reliability of corroding pipelines. International Journal of Pressure Vessels and Piping. 2010 Oct 1;87(10):587-95.

Zhou W, Huang GX. Model error assessments of burst capacity models for corroded pipelines. International Journal of Pressure Vessels and Piping. 2012 Nov 1;99:1-8.

Zhou W, Gong C, Hong H. New perspective on application of first-order reliability method for estimating system reliability. J Eng Mech-ASCE 2017;143(9)

4 Summary, Conclusions and Recommendation for Future Study

4.1 General

This research investigates the characteristics of the pressure of oil pipeline and its impact on reliability analysis. The conclusions drawn from this thesis and recommendations for the future study are given as follows.

4.2 Probabilistic characterization of internal pressure of crude oil transmission pipelines based on pressure records

In chapter 2, statistical characteristics of the discharge and suction pressures based on the minute-by-minute pressure records obtained from a compressor station on an in-service crude oil pipeline was investigated. This pipeline has an MOP of 9.9 MPa and a design factor of 0.8. The discharge and suction pressure records are 1.5 and 1.0 years long, respectively. The probabilistic characteristics of the arbitrary-point-in-time pressure ($p_{d\text{-}apt}$ and $p_{s\text{-}apt}$) as well as the weekly, monthly and annual maximum pressures are derived based on the pressure records for both the discharge and suction pressures. The mean and COV of $p_{d\text{-}apt}$ are evaluated to be 57.3% and 41% MOP, respectively, and the mean and COV of $p_{s\text{-}apt}$ are 13.8%MOP and 71.9%, respectively. The Johnson SB distribution is found to be the best fit distribution for $p_{d\text{-}apt}$ and $p_{s\text{-}apt}$. The monthly and annual maximum discharge pressures can be adequately represented by a deterministic quantity equal to 90%MOP, whereas even the weekly maximum distribution of the discharge pressure could also be considered as deterministic considering the marked drop. The weekly, monthly and annual maximum suction pressures are found to be well characterized by the beta distributions.

The autocorrelation function of the discharge pressure is well fitted by the exponential correlation function with a correlation length equal to 439 minutes, whereas the γ-exponential function

adequately characterizes the autocorrelation function of the suction pressure with a correlation length to be 966 minutes. The analytical expression of the PSD function corresponding to the exponential autocorrelation function for the discharge pressure is obtained and agrees very well with the numerically evaluated PSD function using Welch's method. The PSD function for the suction pressure is also numerically evaluated using Welch's method. The bandwidth parameter α_2 is also calculated for both discharge and suction pressures and indicates that both are wide-band processes. It is found that the Fréchet distributions fit the pressure ranges of the discharge and suction pressures well which are obtained from rainflow counting. The discharge and suction pressure ranges are further compared with the benchmark pressure cycle counts proposed in the literature to identify their severity. The results suggest that the discharge pressure ranges fall in between the very aggressive and aggressive categories, whereas the suction pressure ranges can be characterized as light severity.

4.3 Reliability analyses of corroding pipelines using different approaches to characterize uncertainties in internal pressure

Chapter 3 investigates the reliability of corroded oil pipeline considering arbitrary-point-in-time pressure as stochastic process with multiple reliability methods and compares it with different pressure assumptions. Two examples of oil pipeline with smaller and larger pipe size are chosen with the same MOP and different parameters (wall thickness, diameter, steel grade, etc.). Discharge pressure distribution (Johnson SB) and correlation structure are picked from chapter 2. A spectral representation method ISCM is used to generated discretized pressure in every three hours for five years period where good accuracy is achieved after 5 iterations. Simulation based reliability analysis is compared between pressure as a stochastic process (the benchmark) and extreme value pressure are given where the difference of the failure probability at the end of fifth

year is 29.41% and 29.13% for two cases representing smaller and larger pipe size. Three pressure distributions from several research are also compared using MCS where all of them gives considerably higher failure results than pressure as stochastic process. A major reason is those previously used pressure is considered pipeline operating under MOP while our record is under 0.9 MOP. However, as the upper bound of pressure varies as the operation conditions change, more operating conditions should be implemented as opposed to one to better incorporate the actual environment.

System reliability analysis using FORM proposed by Gong etc. in five years period based on equivalent component method is also calculated and compared with MCS results. FORM analysis shows close results to the benchmark with 1.3% difference using 260-component (5-day interval) for smaller pipe size and -1.2% difference using 30-component (1-month interval) for larger pipe size. The error occurred could be explained by the instantaneous probability, proximity of each equivalent limit state and the number of equivalent components used which all affect the accuracy considerably. However, for extreme value pressure distribution, FORM gives a fairly accurate result comparing with the benchmark with small difference of 27.45% and 5.22% for smaller and larger pipe size. The results give evidence of conservativeness of corrosion failure considering pressure as maximum probable value which is independent of time comparing to pressure as a stochastic process.

4.4 Recommendations for future work

For chapter 2, as the characterized statistics is obtained from the pressure record of a particular pump station within the pipeline system, one upper bound for discharge pressure and one lower bound for suction pressure are observed. However, the bound changes as the operating condition varies. To get a more generous result, more records with different operating conditions including

information about inspection, shutdown etc. and limits like the MOP and lower bound should be incorporated. Distributions that could incorporate those different upper bound should be further investigate. For annual extreme value distribution of the suction pressure which is purely deduced needs more evidence to support the conclusion. For the Welch's method for PSD estimate, the effect of different window function type, overlapping proportion as well as the segment length should be further checked and compared. In addition, the physical meaning about the dominant frequency requires more explanations to describe and suggestions for future uses.

For chapter 3, the failure results from the system FORM are a little deviating from that from the simulation-based result, more research is needed to assess the reason behind. For instantaneous failure, some sensitivity about the impact of the truncated distribution on the instantaneous failure should be checked and furthermore some alternative method that could provide a more accurate method like SORM. Also, the accuracy of the equivalent method with correlation between limit states more than 0.9 should be checked for sensitivity with more components and its limit to obtain acceptable estimates.

Curriculum Vitae

Name:	Yue Liu
Post-secondary Education and Degrees:	Southeast University Nanjing, China 2012-2016 B.Eng. The University of British Columbia Vancouver, BC, Canada 2017-2018 M.Eng. The University of Western Ontario London, Ontario, Canada 2019-2021 M.E.SC
Honours and Awards:	Southeast University course Scholarship 2014, 2015
Related Work Experience	Teaching Assistant The University of Western Ontario 2020-2021